A 3D cutaway diagram of the Mu2e experiment detector. The detector is a long, cylindrical structure with a green outer shell and a blue inner core. A red dashed line represents the particle path through the detector. The detector is mounted on a complex support structure.

Mu2e : An Experimental Search for $\mu^- N \rightarrow e^- N$ at Fermilab

Presented by Sophie Charlotte Middleton

Research Associate at Caltech

Rising Stars in Experimental Particle Physics Symposium

at University of Chicago

September 2021

Charged Lepton Flavor Violation (CLFV)

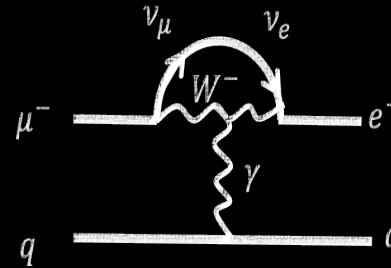
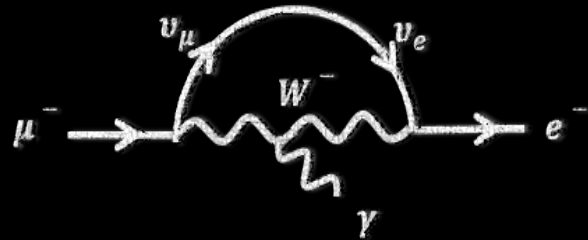


- The minimal extension of the Standard Model, including Dirac masses of neutrinos, allows for CLFV at loop level, mediated by W bosons.



Charged Lepton Flavor Violation (CLFV)

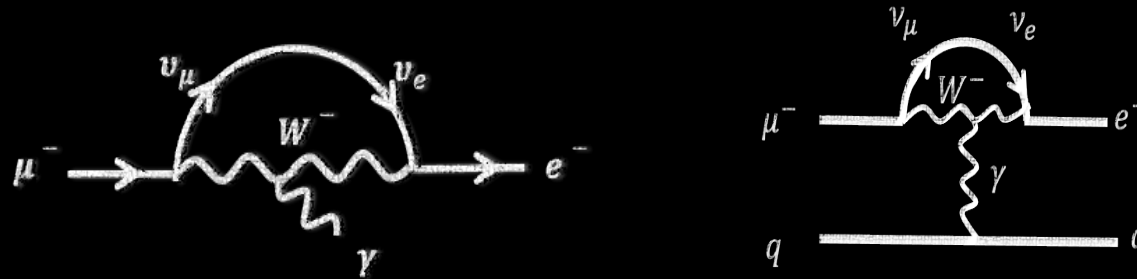
- The minimal extension of the Standard Model, including Dirac masses of neutrinos, allows for CLFV at loop level, mediated by W bosons.





Charged Lepton Flavor Violation (CLFV)

- The minimal extension of the Standard Model, including Dirac masses of neutrinos, allows for CLFV at loop level, mediated by W bosons.

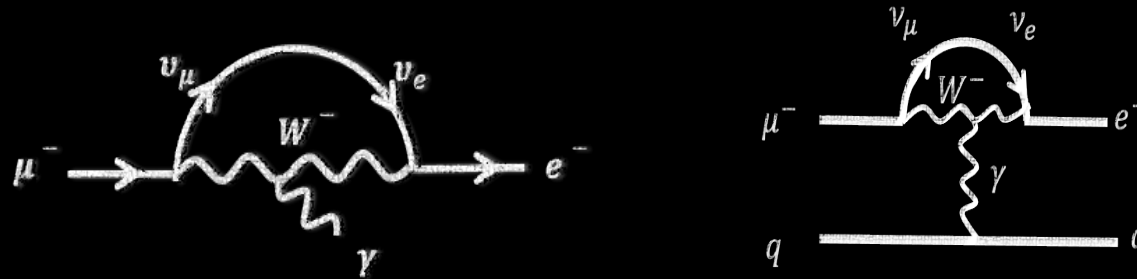


- Rates heavily suppressed by GIM suppression and are far below any conceivable experiment could measure:



Charged Lepton Flavor Violation (CLFV)

- The minimal extension of the Standard Model, including Dirac masses of neutrinos, allows for CLFV at loop level, mediated by W bosons.



- Rates heavily suppressed by GIM suppression and are far below any conceivable experiment could measure:

$$B(\mu \rightarrow e\gamma) = \frac{3\alpha}{32\pi} \left| \sum_{i=2,3} U_{\mu i}^* U_{ei} \frac{\Delta m_{1i}^2}{M_W^2} \right|^2$$

$$B(\mu \rightarrow e\gamma) = \frac{3\alpha}{32\pi} \left(\frac{1}{4} \right) \sin^2 2\theta_{13} \sin^2 \theta_{23} \left| \frac{\Delta m_{13}^2}{M_W^2} \right|^2$$

$$B(\mu \rightarrow e\gamma) \approx \mathcal{O}(10^{-54}) \quad [1-4]$$

using best-fit values for neutrino data ($m_{\nu j}$ for the neutrino mass and U_{ij} for the element of the PMNS matrix).



Charged Lepton Flavor Violation (CLFV)

- The minimal extension of the Standard Model, including Dirac masses of neutrinos, allows for CLFV at loop level, mediated by W bosons.



- Rates heavily suppressed by GIM suppression and are far below any conceivable experiment could measure:

$$B(\mu \rightarrow e\gamma) = \frac{3\alpha}{32\pi} \left| \sum_{i=2,3} U_{\mu i}^* U_{ei} \frac{\Delta m_{1i}^2}{M_W^2} \right|^2$$

$$B(\mu \rightarrow e\gamma) = \frac{3\alpha}{32\pi} \left(\frac{1}{4} \right) \sin^2 2\theta_{13} \sin^2 \theta_{23} \left| \frac{\Delta m_{13}^2}{M_W^2} \right|^2$$

$$B(\mu \rightarrow e\gamma) \approx \mathcal{O}(10^{-54}) \quad [1-4]$$

using best-fit values for neutrino data ($m_{\nu j}$ for the neutrino mass and U_{ij} for the element of the PMNS matrix).

If observed at Mu2e or Mu2e-II → this would be an unambiguous sign of physics beyond the Standard Model (BSM).

BSM Scenarios

Nice overview: Lorenzo Calibbi, Giovanni Signorelli
arXiv:1709.00294 (2018)



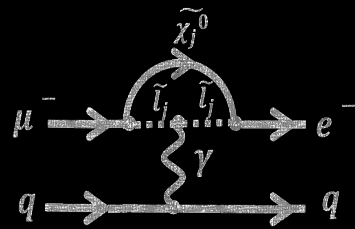
There are many well-motivated BSM theories which invoke CLFV mediated by (pseudo) scalar, (axial) vector, or tensor currents at rates close to current experimental limits i.e. $B \approx 10^{-15} - 10^{-17}$;



BSM Scenarios

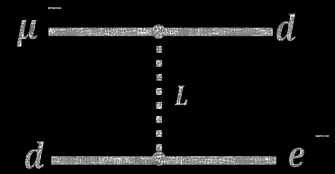
Nice overview: Lorenzo Calibbi, Giovanni Signorelli
arXiv:1709.00294 (2018)

There are many well-motivated BSM theories which invoke CLFV mediated by (pseudo) scalar, (axial) vector, or tensor currents at rates close to current experimental limits i.e. $B \approx 10^{-15} - 10^{-17}$:



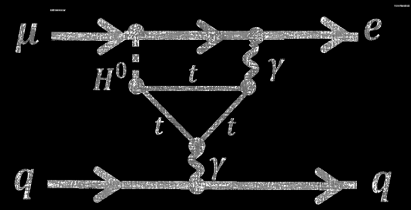
SO(10) SUSY :
L. Calibbi *et al.*, Phys. Rev. D **74**, 116002 (2006), L. Calibbi *et al.*, JHEP **1211**, 40 (2012).

Scalar Leptoquarks:
J.M. Arnold *et al.*, Phys. Rev D **88**, 035009 (2013).



Different neutrino mass-generating Lagrangians lead to very different rates for CLFV :
Nuclear Physics B (Proc. Suppl.) **248-250** (2014) 13-19

Extended Higgs/Gauge sector:
Left-Right Symmetric Models
C.-H. Lee *et al.*, Phys. Rev D **88**, 093010 (2013).
Littlest Higgs Blanke *et al* Phys.Polon.B41:657, 2010, arXiv:0906.5454v2 [hep-ph]

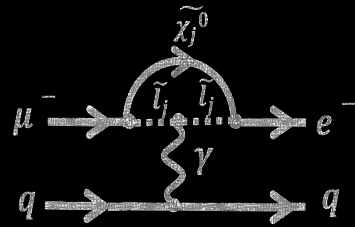




Nice overview: Lorenzo Calibbi, Giovanni Signorelli
arXiv:1709.00294 (2018)

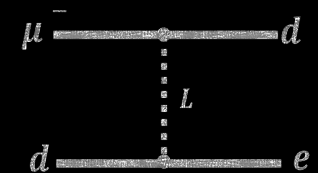
BSM Scenarios

There are many well-motivated BSM theories which invoke CLFV mediated by (pseudo) scalar, (axial) vector, or tensor currents at rates close to current experimental limits i.e. $B \approx 10^{-15} - 10^{-17}$;



SO(10) SUSY :
L. Calibbi *et al.*, Phys. Rev. D **74**, 116002 (2006), L. Calibbi *et al.*, JHEP **1211**, 40 (2012).

Scalar Leptoquarks:
J.M. Arnold *et al.*, Phys. Rev D **88**, 035009 (2013).



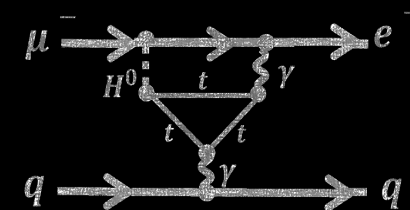
A few examples – not an exclusive list!

Important point:

Mu2e is an indirect search for new physics, with sensitivity to lots of models. Even a null result would have huge implications!

Different neutrino mass-generating Lagrangians lead to very different rates for CLFV :
Nuclear Physics B (Proc. Suppl.) **248–250** (2014) 13–19

Extended Higgs/Gauge sector:
Left-Right Symmetric Models
C.-H. Lee *et al.*, Phys. Rev D **88**, 093010 (2013).
Littlest Higgs Blanke *et al* Phys.Polon.B41:657, 2010, arXiv:0906.5454v2 [hep-ph]

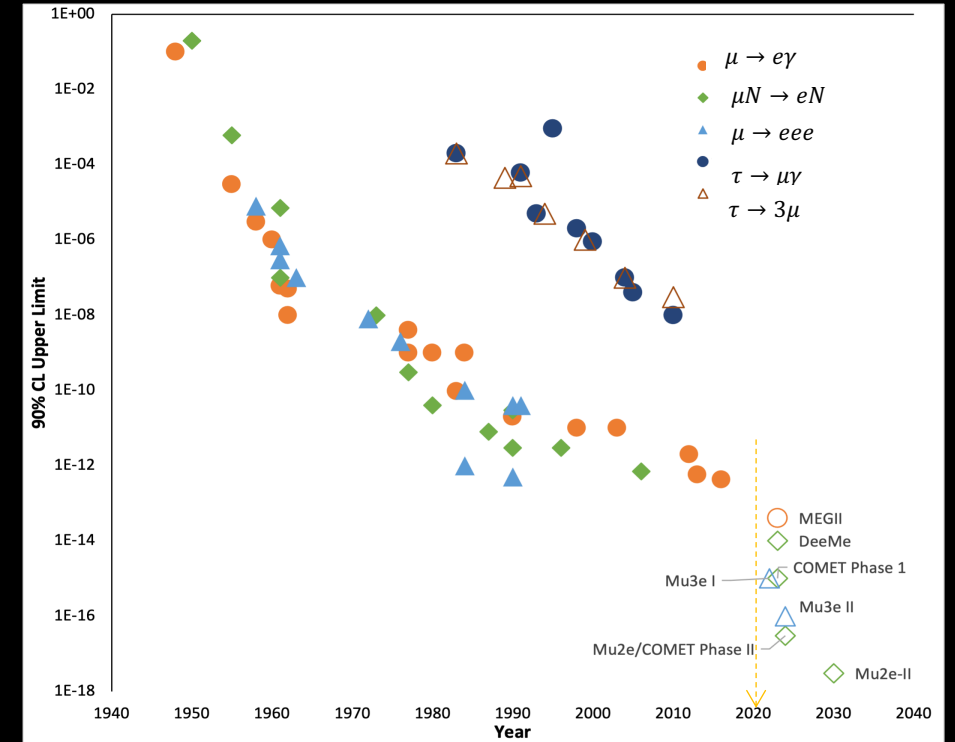


Experimental Searches for CLFV



- $\mu^- N \rightarrow e^- N$ searches are crucial part of global program searching for CLFV.
- Muons offer more powerful probe for CLFV compared to taus.
- To elucidate the mechanism responsible for any CLFV – must look at relative rates (if any) in different muon channels.

Mode	Current Limit (at 90% CL)	Future Proposed Limit	Future Experiment/s
$\mu^\pm \rightarrow e^\pm \gamma$	4.2×10^{-13} [5]	4×10^{-14}	MEG II [8]
$\mu^- N \rightarrow e^- N$	7×10^{-13} [6]	10^{-15} 10^{-17} 10^{-18}	COMET Phase-I Mu2e [10] & COMET Phase-II [9] Mu2e-II
$\mu^+ \rightarrow e^+ e^+ e^-$	$\sim 10^{-12}$ [7]	$10^{-15} \sim 10^{-16}$	Mu3e



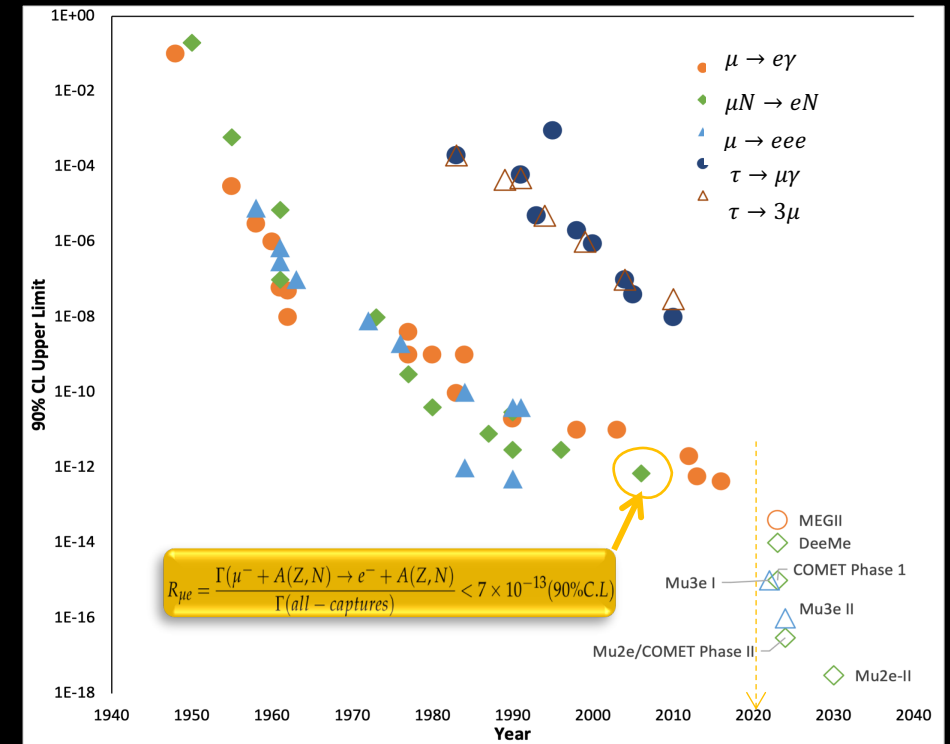
- Muon-to-electron sector provides powerful probes and complements collider searches for $\tau \rightarrow e\gamma$ or $\mu\gamma$ and $H \rightarrow e\tau$, $\mu\tau$, or μe .

Experimental Searches for CLFV



- $\mu^- N \rightarrow e^- N$ searches are crucial part of global program searching for CLFV.
- Muons offer more powerful probe for CLFV compared to taus.
- To elucidate the mechanism responsible for any CLFV – must look at relative rates (if any) in different muon channels.

Mode	Current Limit (at 90% CL)	Future Proposed Limit	Future Experiment/s
$\mu^\pm \rightarrow e^\pm \gamma$	4.2×10^{-13} [5]	4×10^{-14}	MEG II [8]
$\mu^- N \rightarrow e^- N$	7×10^{-13} [6]	10^{-15} 10^{-17} 10^{-18}	COMET Phase-I Mu2e [10] & COMET Phase-II [9] Mu2e-II
$\mu^+ \rightarrow e^+ e^+ e^-$	$\sim 10^{-12}$ [7]	$10^{-15} \sim 10^{-16}$	Mu3e



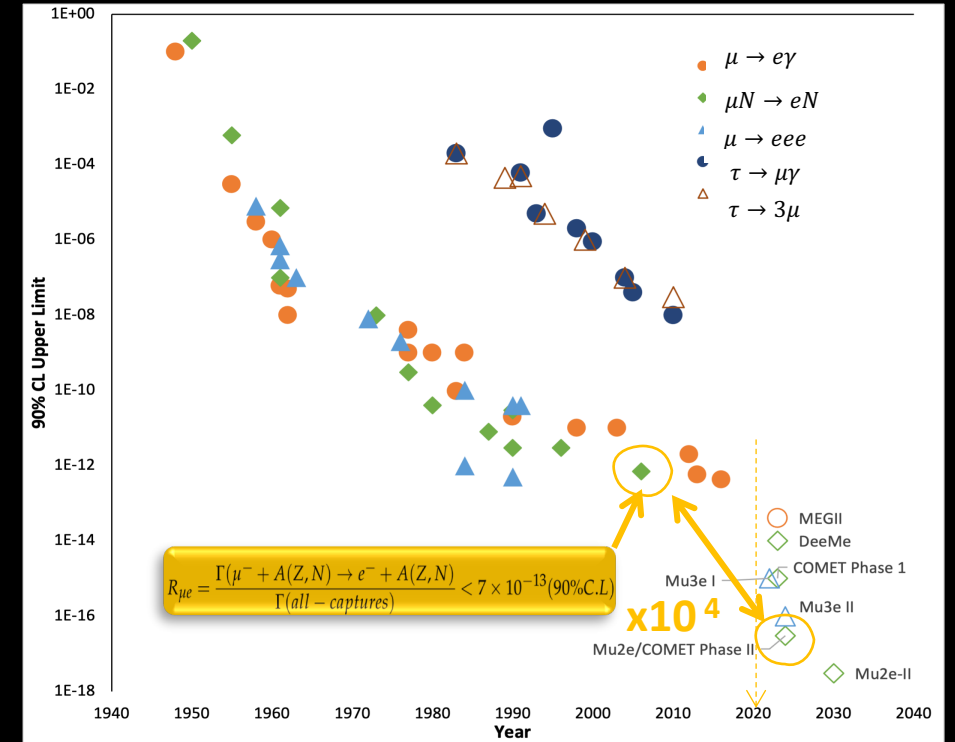
- Muon-to-electron sector provides powerful probes and complements collider searches for $\tau \rightarrow e\gamma$ or $\mu\gamma$ and $H \rightarrow e\tau$, $\mu\tau$, or μe .

Experimental Searches for CLFV



- $\mu^- N \rightarrow e^- N$ searches are crucial part of global program searching for CLFV.
- Muons offer more powerful probe for CLFV compared to taus.
- To elucidate the mechanism responsible for any CLFV – must look at relative rates (if any) in different muon channels.

Mode	Current Limit (at 90% CL)	Future Proposed Limit	Future Experiment/s
$\mu^\pm \rightarrow e^\pm \gamma$	4.2×10^{-13} [5]	4×10^{-14}	MEG II [8]
$\mu^- N \rightarrow e^- N$	7×10^{-13} [6]	10^{-15} 10^{-17} 10^{-18}	COMET Phase-I Mu2e [10] & COMET Phase-II [9] Mu2e-II
$\mu^+ \rightarrow e^+ e^+ e^-$	$\sim 10^{-12}$ [7]	$10^{-15} \sim 10^{-16}$	Mu3e



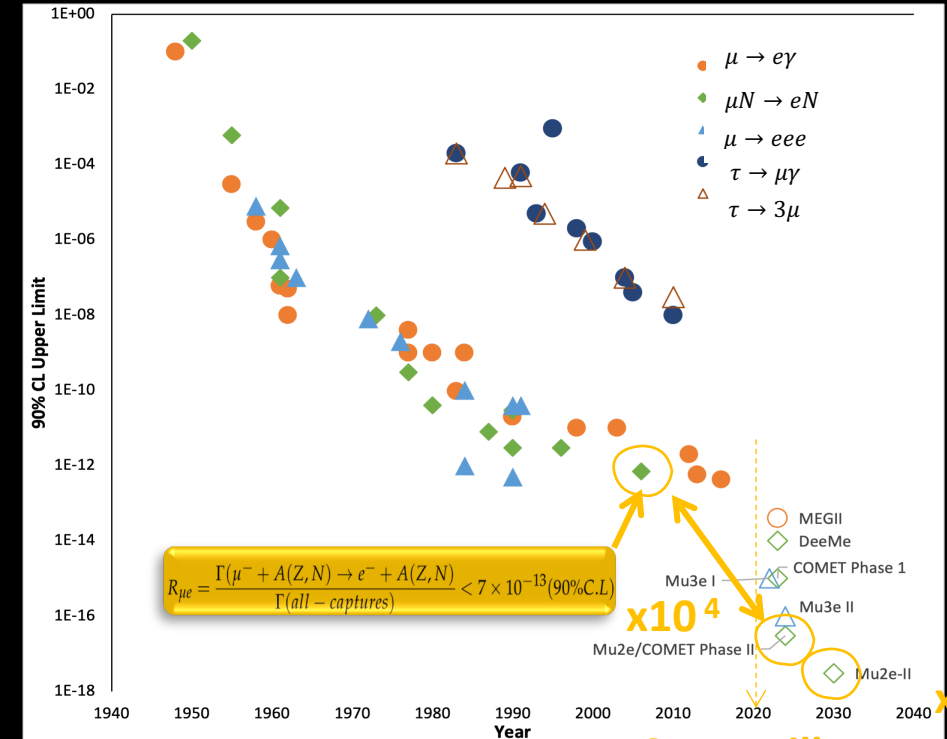
- Muon-to-electron sector provides powerful probes and complements collider searches for $\tau \rightarrow e\gamma$ or $\mu\gamma$ and $H \rightarrow e\tau$, $\mu\tau$, or μe .

Experimental Searches for CLFV



- $\mu^- N \rightarrow e^- N$ searches are crucial part of global program searching for CLFV.
- Muons offer more powerful probe for CLFV compared to taus.
- To elucidate the mechanism responsible for any CLFV – must look at relative rates (if any) in different muon channels.

Mode	Current Limit (at 90% CL)	Future Proposed Limit	Future Experiment/s
$\mu^\pm \rightarrow e^\pm \gamma$	4.2×10^{-13} [5]	4×10^{-14}	MEG II [8]
$\mu^- N \rightarrow e^- N$	7×10^{-13} [6]	10^{-15} 10^{-17} 10^{-18}	COMET Phase-I Mu2e [10] & COMET Phase-II [9] Mu2e-II
$\mu^+ \rightarrow e^+ e^+ e^-$	$\sim 10^{-12}$ [7]	$10^{-15} \sim 10^{-16}$	Mu3e



Mu2e-II will use PIP-II, Snowmass Proposal in progress!

- Muon-to-electron sector provides powerful probes and complements collider searches for $\tau \rightarrow e\gamma$ or $\mu\gamma$ and $H \rightarrow e\tau$, $\mu\tau$, or μe .



Simplistic Explanation of Physics Reach

A. de Gouvêa, P. Vogel
arXiv:1303.4097

- For the purposes of discussion we can build a Toy Lagrangian which consists of 2 terms representing 2 types of physics process:

$$\mathcal{L}_{CLFV} = \frac{m_\mu}{(1 + \kappa)\Lambda^2} \bar{\mu}_R \sigma_{\mu\nu} e_L F^{\mu\nu} + \frac{\kappa}{(1 + \kappa)\Lambda^2} \bar{\mu}_L \gamma_\mu e_L \left(\sum_{q=u,d} \bar{q}_L \gamma_\mu q_L \right)$$



A. de Gouvêa, P. Vogel
arXiv:1303.4097

Simplistic Explanation of Physics Reach

- For the purposes of discussion we can build a Toy Lagrangian which consists of 2 terms representing 2 types of physics process:

$$\mathcal{L}_{CLFV} = \frac{m_\mu}{(1+\kappa)\Lambda^2} \bar{\mu}_R \sigma_{\mu\nu} e_L F^{\mu\nu} + \frac{\kappa}{(1+\kappa)\Lambda^2} \bar{\mu}_L \gamma_\mu e_L \left(\sum_{q=u,d} \bar{q}_L \gamma_\mu q_L \right)$$

“Photonic”



Λ : effective mass scale of New Physics (NP),
 κ : determines to what extent NP is photonic ($\kappa \ll 1$) or 4-fermion ($\kappa \gg 1$)



Simplistic Explanation of Physics Reach

A. de Gouvêa, P. Vogel
arXiv:1303.4097

- For the purposes of discussion we can build a Toy Lagrangian which consists of 2 terms representing 2 types of physics process:

$$\mathcal{L}_{CLFV} = \frac{m_\mu}{(1 + \kappa)\Lambda^2} \bar{\mu}_R \sigma_{\mu\nu} e_L F^{\mu\nu} + \frac{\kappa}{(1 + \kappa)\Lambda^2} \bar{\mu}_L \gamma_\mu e_L \left(\sum_{q=u,d} \bar{q}_L \gamma_\mu q_L \right)$$

“Photonic”
i.e. Dipole terms:
 $\mu^\pm \rightarrow e^\pm \gamma$, $\mu \rightarrow eee$
 $\mu^- N \rightarrow e^- N$



Λ : effective mass scale of New Physics (NP),
 κ : determines to what extent NP is photonic ($\kappa \ll 1$) or 4-fermion ($\kappa \gg 1$)



Simplistic Explanation of Physics Reach

A. de Gouvêa, P. Vogel
arXiv:1303.4097

- For the purposes of discussion we can build a Toy Lagrangian which consists of 2 terms representing 2 types of physics process:

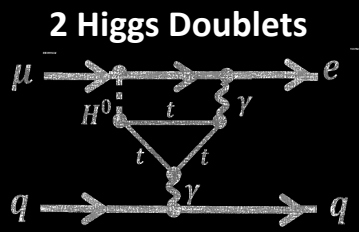
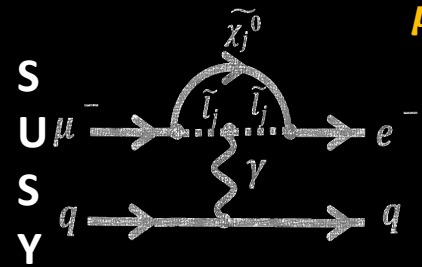
$$\mathcal{L}_{CLFV} = \frac{m_\mu}{(1 + \kappa)\Lambda^2} \bar{\mu}_R \sigma_{\mu\nu} e_L F^{\mu\nu} + \frac{\kappa}{(1 + \kappa)\Lambda^2} \bar{\mu}_L \gamma_\mu e_L \left(\sum_{q=u,d} \bar{q}_L \gamma_\mu q_L \right)$$

“Photonic”

i.e. Dipole terms:

$$\mu^\pm \rightarrow e^\pm \gamma, \mu \rightarrow e e e$$

$$\mu^- N \rightarrow e^- N$$



Λ : effective mass scale of New Physics (NP),

κ : determines to what extent NP is photonic ($\kappa \ll 1$) or 4-fermion ($\kappa \gg 1$)



Simplistic Explanation of Physics Reach

A. de Gouvêa, P. Vogel
arXiv:1303.4097

- For the purposes of discussion we can build a Toy Lagrangian which consists of 2 terms representing 2 types of physics process:

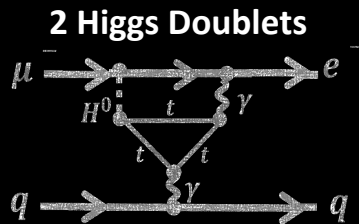
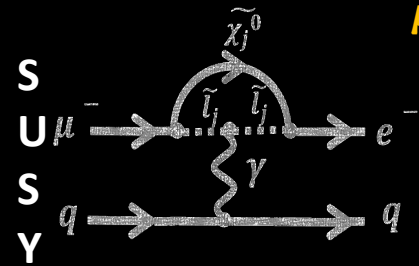
$$\mathcal{L}_{CLFV} = \frac{m_\mu}{(1 + \kappa)\Lambda^2} \bar{\mu}_R \sigma_{\mu\nu} e_L F^{\mu\nu} + \frac{\kappa}{(1 + \kappa)\Lambda^2} \bar{\mu}_L \gamma_\mu e_L \left(\sum_{q=u,d} \bar{q}_L \gamma_\mu q_L \right)$$

“Photonic”

i.e. Dipole terms:

$$\mu^\pm \rightarrow e^\pm \gamma, \mu \rightarrow eee$$

$$\mu^- N \rightarrow e^- N$$



“Contact”

i.e. 4 fermion terms

$$\text{Only } \mu^+ \rightarrow e^+ e^+ e^-$$

$$\text{And } \mu^- N \rightarrow e^- N$$

Λ : effective mass scale of New Physics (NP),

κ : determines to what extent NP is photonic ($\kappa \ll 1$) or 4-fermion ($\kappa \gg 1$)



Simplistic Explanation of Physics Reach

A. de Gouvêa, P. Vogel
arXiv:1303.4097

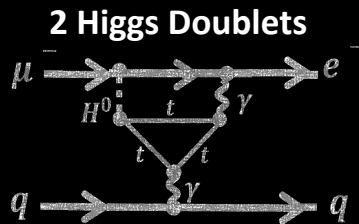
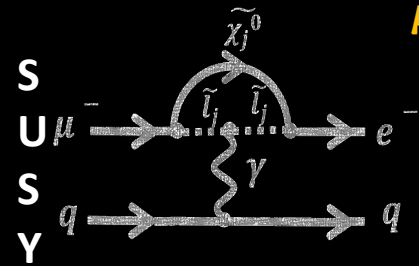
- For the purposes of discussion we can build a Toy Lagrangian which consists of 2 terms representing 2 types of physics process:

$$\mathcal{L}_{CLFV} = \frac{m_\mu}{(1 + \kappa)\Lambda^2} \bar{\mu}_R \sigma_{\mu\nu} e_L F^{\mu\nu} + \frac{\kappa}{(1 + \kappa)\Lambda^2} \bar{\mu}_L \gamma_\mu e_L \left(\sum_{q=u,d} \bar{q}_L \gamma_\mu q_L \right)$$

“Photonic”

i.e. Dipole terms:

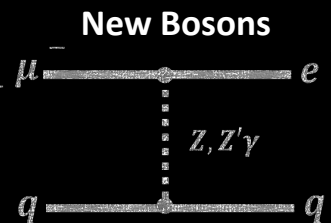
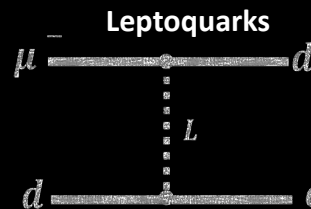
$\mu^\pm \rightarrow e^\pm \gamma$, $\mu \rightarrow eee$
 $\mu^- N \rightarrow e^- N$



“Contact”

i.e. 4 fermion terms

Only $\mu^+ \rightarrow e^+ e^+ e^-$
And $\mu^- N \rightarrow e^- N$



Λ : effective mass scale of New Physics (NP),

κ : determines to what extent NP is photonic ($\kappa \ll 1$) or 4-fermion ($\kappa \gg 1$)

Simplistic Explanation of Physics Reach



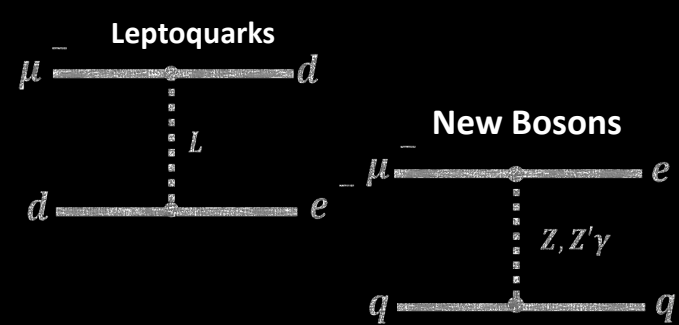
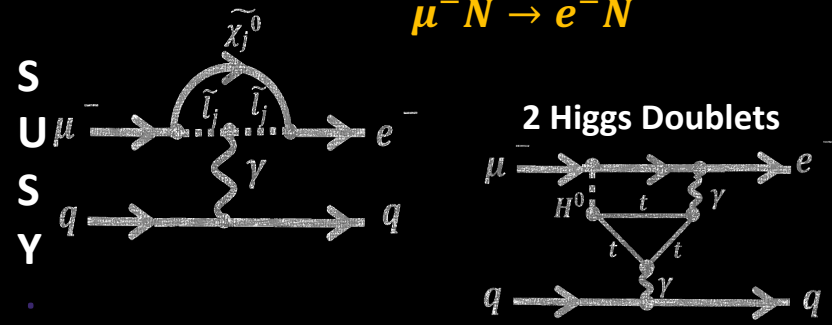
A. de Gouvêa, P. Vogel
arXiv:1303.4097

- For the purposes of discussion we can build a Toy Lagrangian which consists of 2 terms representing 2 types of physics process:

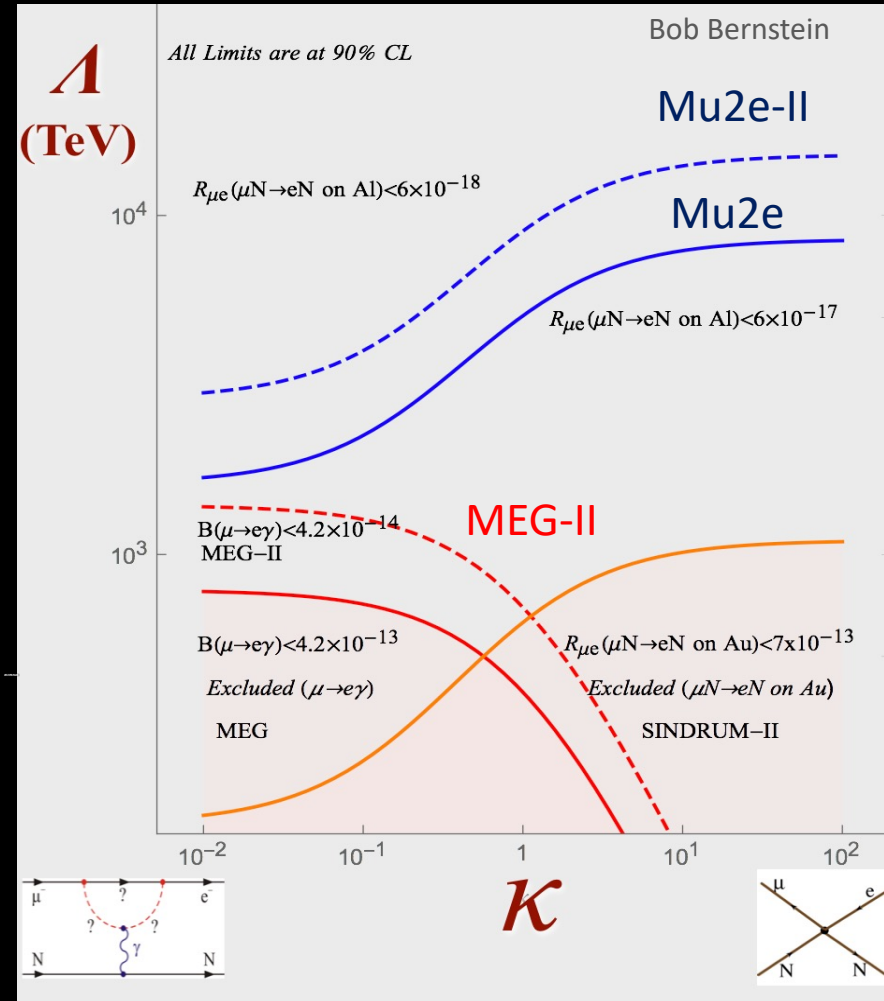
$$\mathcal{L}_{CLFV} = \frac{m_\mu}{(1 + \kappa)\Lambda^2} \bar{\mu}_R \sigma_{\mu\nu} e_L F^{\mu\nu} + \frac{\kappa}{(1 + \kappa)\Lambda^2} \bar{\mu}_L \gamma_\mu e_L \left(\sum_{q=u,d} \bar{q}_L \gamma_\mu q_L \right)$$

“Photonic”
i.e. Dipole terms:
 $\mu^\pm \rightarrow e^\pm \gamma, \mu \rightarrow eee$
 $\mu^- N \rightarrow e^- N$

“Contact”
i.e. 4 fermion terms
Only $\mu^+ \rightarrow e^+ e^+ e^-$
And $\mu^- N \rightarrow e^- N$



Λ : effective mass scale of New Physics (NP),
 κ : determines to what extent NP is photonic ($\kappa \ll 1$) or 4-fermion ($\kappa \gg 1$)



Complementarity



Taken from: arXiv:0909.1333[hep-ph]

	AC	RVV2	AKM	δ LL	FBMSSM	LHT	RS
$D^0 - \bar{D}^0$	★★★★	★	★	★	★	★★★★	?
ϵ_K	★	★★★★	★★★★	★	★	★★	★★★★
$S_{\psi\phi}$	★★★★	★★★★	★★★★	★	★	★★★★	★★★★
$S_{\phi K_S}$	★★★★	★★	★	★★★★	★★★★	★	?
$A_{CP}(B \rightarrow X_s \gamma)$	★	★	★	★★★★	★★★★	★	?
$A_{7,8}(B \rightarrow K^* \mu^+ \mu^-)$	★	★	★	★★★★	★★★★	★★	?
$A_9(B \rightarrow K^* \mu^+ \mu^-)$	★	★	★	★	★	★	?
$B \rightarrow K^{(*)} \nu \bar{\nu}$	★	★	★	★	★	★	★
$B_s \rightarrow \mu^+ \mu^-$	★★★★	★★★★	★★★★	★★★★	★★★★	★	★
$K^+ \rightarrow \pi^+ \nu \bar{\nu}$	★	★	★	★	★	★★★★	★★★★
$K_L \rightarrow \pi^0 \nu \bar{\nu}$	★	★	★	★	★	★★★★	★★★★
$\mu \rightarrow e \gamma$	★★★★	★★★★	★★★★	★★★★	★★★★	★★★★	★★★★
$\tau \rightarrow \mu \gamma$	★★★★	★★★★	★	★★★★	★★★★	★★★★	★★★★
$\mu + N \rightarrow e + N$	★★★★	★★★★	★★★★	★★★★	★★★★	★★★★	★★★★

Table 8: "DNA" of flavour physics effects for the most interesting observables in a selection of SUSY and non-SUSY models ★★★★★ signals large effects, ★★ visible but small effects and ★ implies that the given model does not predict sizable effects in that observable.

★★★★ = Discovery Sensitivity

Complementarity



Taken from: arXiv:0909.1333[hep-ph]

	AC	RVV2	AKM	δLL	FBMSSM	LHT	RS
$D^0 - \bar{D}^0$	★★★★	★	★	★	★	★★★★	?
ϵ_K	★	★★★★	★★★★	★	★	★★	★★★★
$S_{\psi\phi}$	★★★★	★★★★	★★★★	★	★	★★★★	★★★★
$S_{\phi K_S}$	★★★★	★★	★	★★★★	★★★★	★	?
$A_{CP}(B \rightarrow X_s \gamma)$	★	★	★	★★★★	★★★★	★	?
$A_{7,8}(B \rightarrow K^* \mu^+ \mu^-)$	★	★	★	★★★★	★★★★	★★	?
$A_9(B \rightarrow K^* \mu^+ \mu^-)$	★	★	★	★	★	★	?
$B \rightarrow K^{(*)} \nu \bar{\nu}$	★	★	★	★	★	★	★
$B_s \rightarrow \mu^+ \mu^-$	★★★★	★★★★	★★★★	★★★★	★★★★	★	★
$K^+ \rightarrow \pi^+ \nu \bar{\nu}$	★	★	★	★	★	★★★★	★★★★
$K_L \rightarrow \pi^0 \nu \bar{\nu}$	★	★	★	★	★	★★★★	★★★★
$\mu \rightarrow e \gamma$	★★★★	★★★★	★★★★	★★★★	★★★★	★★★★	★★★★
$\tau \rightarrow \mu \gamma$	★★★★	★★★★	★	★★★★	★★★★	★★★★	★★★★
$\mu + N \rightarrow e + N$	★★★★	★★★★	★★★★	★★★★	★★★★	★★★★	★★★★

★★★★ = Discovery Sensitivity

Table 8: "DNA" of flavour physics effects for the most interesting observables in a selection of SUSY and non-SUSY models ★★★★★ signals large effects, ★★ visible but small effects and ★ implies that the given model does not predict sizable effects in that observable.

Discovery sensitivity across the board. Relative Rates however will be model dependent.

Complementarity



Taken from: arXiv:0909.1333[hep-ph]

	AC	RVV2	AKM	δ LL	FBMSSM	LHT	RS
$D^0 - \bar{D}^0$	★★★★	★	★	★	★	★★★★	?
ϵ_K	★	★★★★	★★★★	★	★	★★	★★★★
$S_{\psi\phi}$	★★★★	★★★★	★★★★	★	★	★★★★	★★★★
$S_{\phi K_S}$	★★★★	★★	★	★★★★	★★★★	★	?
$A_{CP}(B \rightarrow X_s \gamma)$	★	★	★	★★★★	★★★★	★	?
$A_{7,8}(B \rightarrow K^* \mu^+ \mu^-)$	★	★	★	★★★★	★★★★	★★	?
$A_9(B \rightarrow K^* \mu^+ \mu^-)$	★	★	★	★	★	★	?
$B \rightarrow K^{(*)} \nu \bar{\nu}$	★	★	★	★	★	★	★
$B_s \rightarrow \mu^+ \mu^-$	★★★★	★★★★	★★★★	★★★★	★★★★	★	★
$K^+ \rightarrow \pi^+ \nu \bar{\nu}$	★	★	★	★	★	★★★★	★★★★
$K_L \rightarrow \pi^0 \nu \bar{\nu}$	★	★	★	★	★	★★★★	★★★★
$\mu \rightarrow e \gamma$	★★★★	★★★★	★★★★	★★★★	★★★★	★★★★	★★★★
$\tau \rightarrow \mu \gamma$	★★★★	★★★★	★	★★★★	★★★★	★★★★	★★★★
$\mu + N \rightarrow e + N$	★★★★	★★★★	★★★★	★★★★	★★★★	★★★★	★★★★

★★★★ = Discovery Sensitivity

Table 8: “DNA” of flavour physics effects for the most interesting observables in a selection of SUSY and non-SUSY models ★★★★★ signals large effects, ★★ visible but small effects and ★ implies that the given model does not predict sizable effects in that observable.

Discovery sensitivity across the board. Relative Rates however will be model dependent.

Model	$\mu \rightarrow eee$	$\mu N \rightarrow eN$	$\frac{BR(\mu \rightarrow eee)}{BR(\mu \rightarrow e \gamma)}$	$\frac{CR(\mu N \rightarrow eN)}{BR(\mu \rightarrow e \gamma)}$
MSSM	Loop	Loop	$\approx 6 \times 10^{-3}$	$10^{-3} - 10^{-2}$
Type-I seesaw	Loop*	Loop*	$3 \times 10^{-3} - 0.3$	0.1–10
Type-II seesaw	Tree	Loop	$(0.1 - 3) \times 10^3$	$\mathcal{O}(10^{-2})$
Type-III seesaw	Tree	Tree	$\approx 10^3$	$\mathcal{O}(10^3)$
LFV Higgs	Loop [†]	Loop* [†]	$\approx 10^{-2}$	$\mathcal{O}(0.1)$
Composite Higgs	Loop*	Loop*	0.05 – 0.5	2 – 20

from L. Calibbi and G. Signorelli, Riv. Nuovo Cimento, 41 (2018) 71

arXiv:1709.00294v2[hep-ph]

Complementarity



Taken from: arXiv:0909.1333[hep-ph]

	AC	RVV2	AKM	δ LL	FBMSSM	LHT	RS
$D^0 - \bar{D}^0$	★★★★	★	★	★	★	★★★★	?
ϵ_K	★	★★★★	★★★★	★	★	★★	★★★★
$S_{\psi\phi}$	★★★★	★★★★	★★★★	★	★	★★★★	★★★★
$S_{\phi K_S}$	★★★★	★★	★	★★★★	★★★★	★	?
$A_{CP}(B \rightarrow X_s \gamma)$	★	★	★	★★★★	★★★★	★	?
$A_{7,8}(B \rightarrow K^* \mu^+ \mu^-)$	★	★	★	★★★★	★★★★	★★	?
$A_9(B \rightarrow K^* \mu^+ \mu^-)$	★	★	★	★	★	★	?
$B \rightarrow K^{(*)} \nu \bar{\nu}$	★	★	★	★	★	★	★
$B_s \rightarrow \mu^+ \mu^-$	★★★★	★★★★	★★★★	★★★★	★★★★	★	★
$K^+ \rightarrow \pi^+ \nu \bar{\nu}$	★	★	★	★	★	★★★★	★★★★
$K_L \rightarrow \pi^0 \nu \bar{\nu}$	★	★	★	★	★	★★★★	★★★★
$\mu \rightarrow e \gamma$	★★★★	★★★★	★★★★	★★★★	★★★★	★★★★	★★★★
$\tau \rightarrow \mu \gamma$	★★★★	★★★★	★	★★★★	★★★★	★★★★	★★★★
$\mu + N \rightarrow e + N$	★★★★	★★★★	★★★★	★★★★	★★★★	★★★★	★★★★

★★★★ = Discovery Sensitivity

Table 8: “DNA” of flavour physics effects for the most interesting observables in a selection of SUSY and non-SUSY models ★★★★★ signals large effects, ★★ visible but small effects and ★ implies that the given model does not predict sizable effects in that observable.

Discovery sensitivity across the board. Relative Rates however will be model dependent.

Model	$\mu \rightarrow eee$	$\mu N \rightarrow eN$	$\frac{BR(\mu \rightarrow eee)}{BR(\mu \rightarrow e \gamma)}$	$\frac{CR(\mu N \rightarrow eN)}{BR(\mu \rightarrow e \gamma)}$
MSSM	Loop	Loop	$\approx 6 \times 10^{-3}$	$10^{-3} - 10^{-2}$
Type-I seesaw	Loop*	Loop*	$3 \times 10^{-3} - 0.3$	0.1–10
Type-II seesaw	Tree	Loop	$(0.1 - 3) \times 10^3$	$\mathcal{O}(10^{-2})$
Type-III seesaw	Tree	Tree	$\approx 10^3$	$\mathcal{O}(10^3)$
LFV Higgs	Loop [†]	Loop* [†]	$\approx 10^{-2}$	$\mathcal{O}(0.1)$
Composite Higgs	Loop*	Loop*	0.05 – 0.5	2 – 20

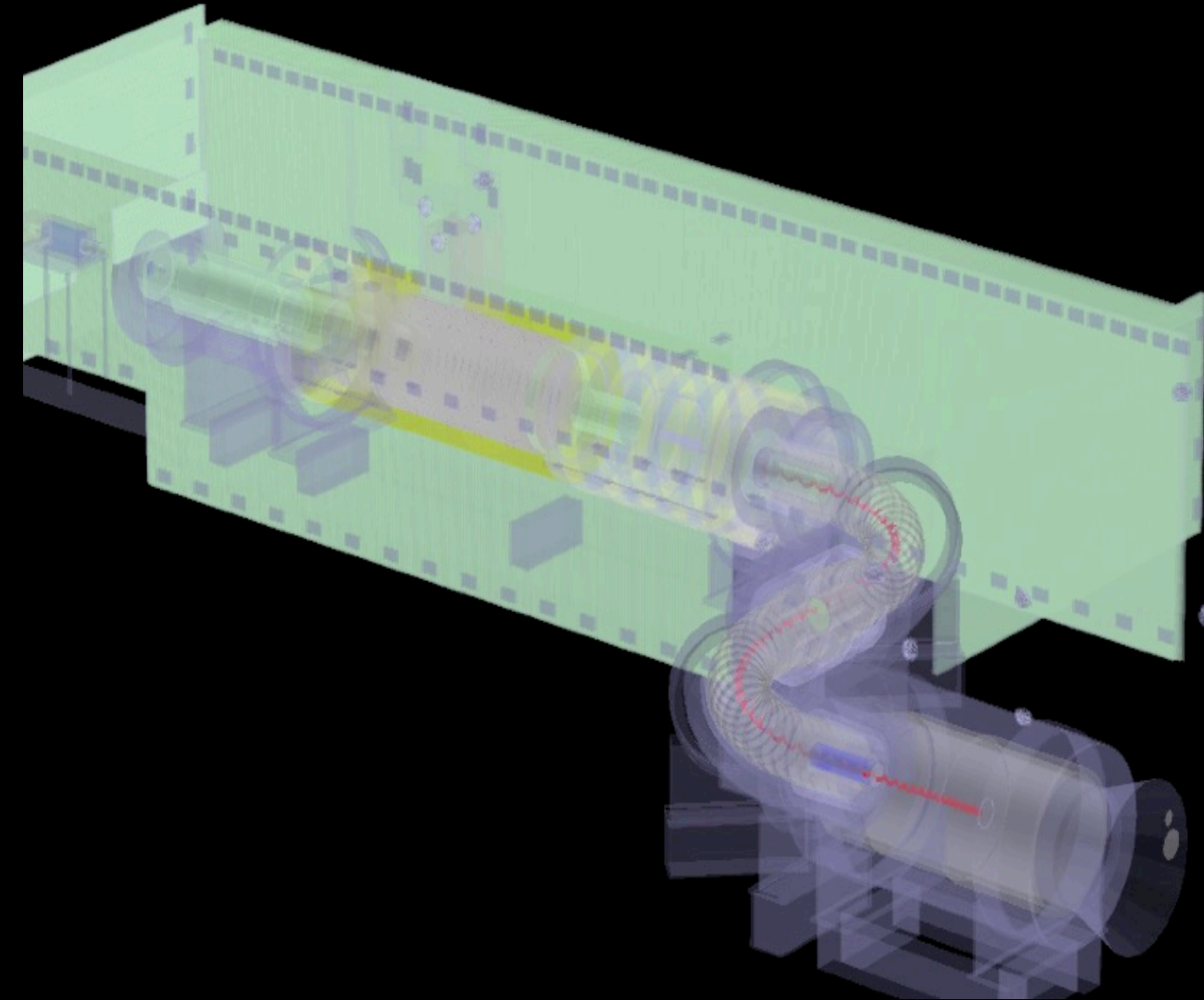
from L. Calibbi and G. Signorelli, Riv. Nuovo Cimento, 41 (2018) 71

arXiv:1709.00294v2[hep-ph]



Experimental Strategy

How will Mu2e try to measure this process?





Muonic Atoms

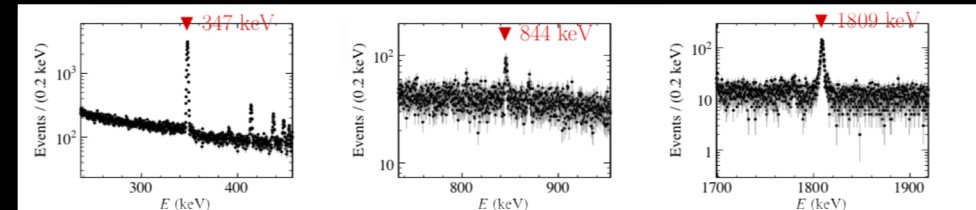
- The $\mu \rightarrow e$ conversion rate is measured as a ratio to the muon capture rate on the same nucleus:

$$R_{\mu e} = \frac{\Gamma(\mu^- + A(Z, N) \rightarrow e^- + A(Z, N))}{\Gamma(\text{all-captures})}$$

- Low momentum (-) muons are captured in the target atomic orbit and quickly (\sim fs) cascades to 1s state.
- Lifetime of muonic aluminium = 864 ns
- In aluminum:

Normalization = from X-rays emitted when muon stops in Al.

- 39 % Decay** : $\mu + N \rightarrow e + \bar{\nu}_e + \nu_\mu$ (**Background**)
- 61 % Capture** : $\mu + N \rightarrow \nu_\mu + N'$ (**Normalization**)
- The Signal** : $\mu + N \rightarrow e + N$ (**Conversion**)



- Signal is monoenergetic electron consistent with:

$$E_e = m_\mu - E_{recoil} - E_{1SB.E}, \text{ e.g For Al: } E_e = 104.97 \text{ MeV.}$$

- Will be smeared by detector and stopping target effects.
- Nucleus coherently recoils off outgoing electron; it does not break-up!

Mu2e gets 8kW, 8GeV Protons from the Fermilab booster:

- Mu2e will acquire ϑ (10^{20}) Protons on Target to achieve design goal

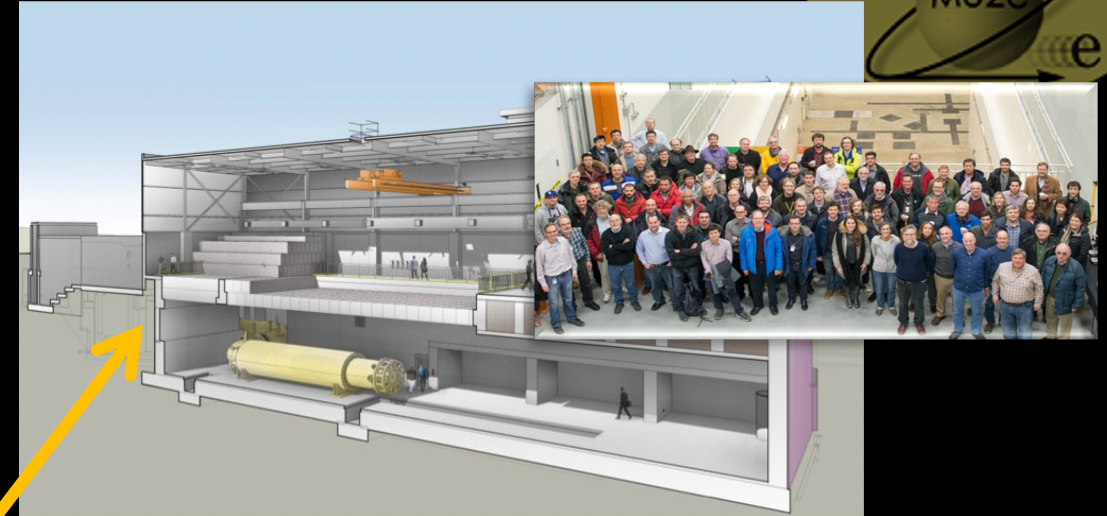


Mu2e gets 8kW, 8GeV Protons from the Fermilab booster:

- Mu2e will acquire ϑ (10^{20}) Protons on Target to achieve design goal



Mu2e building:



Mu2e gets 8kW, 8GeV Protons from the Fermilab booster:

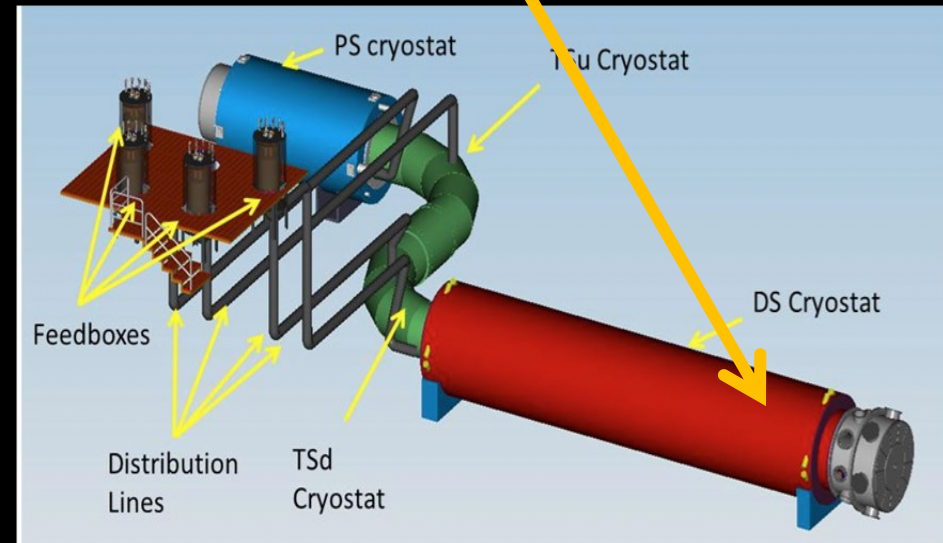
- Mu2e will acquire ϑ (10^{20}) Protons on Target to achieve design goal



Mu2e building:



Mu2e:

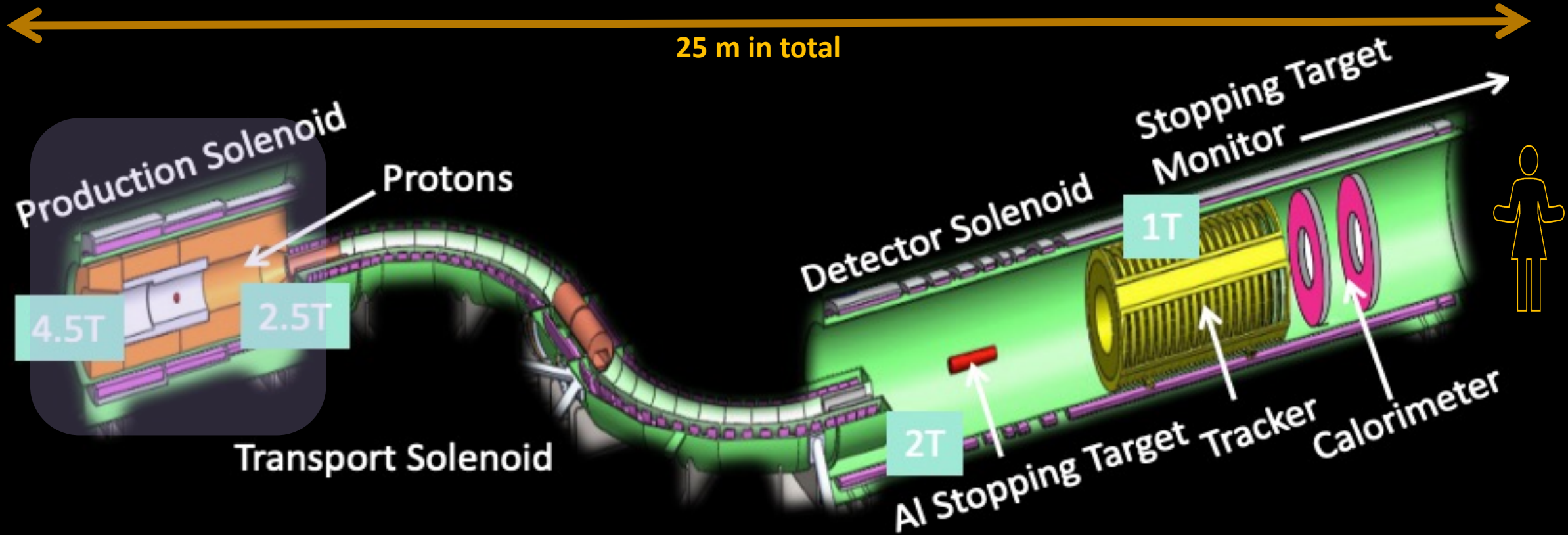


The Mu2e Experiment

V. Lobashev & R. Djilkibaev (Sov. J. Nucl. Phys. 49(2), 384 (1989))



- Production Solenoid:**
- 8 GeV Protons enter, pions produced, decay to muons
 - Graded magnetic field reflects pions/muons to transport solenoid



The Mu2e Experiment

V. Lobashev & R. Djilkibaev (Sov. J. Nucl. Phys. 49(2), 384 (1989))



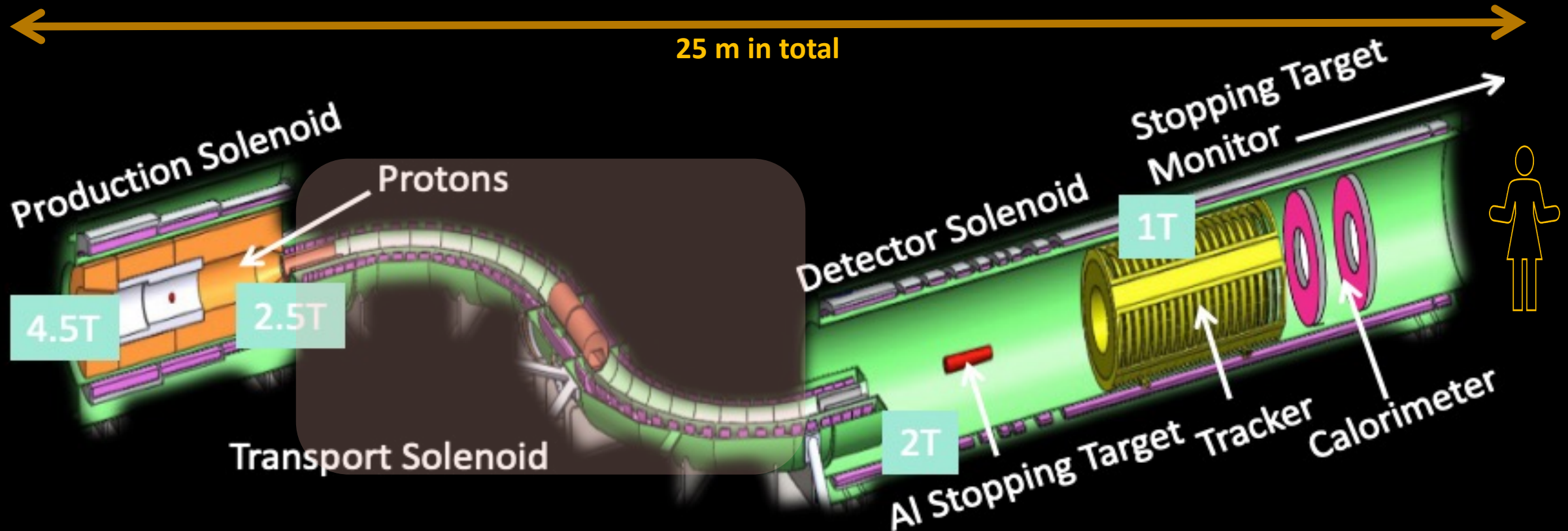
Production Solenoid:

- 8 GeV Protons enter, pions produced, decay to muons
- Graded magnetic field reflects pions/muons to transport solenoid

Transport Solenoid:

- “S” shape removes line of sight backgrounds
- Windows remove anti-protons
- Collimators help select low momentum, negative muons and “focus” on detector solenoid aperture.

25 m in total



The Mu2e Experiment

V. Lobashev & R. Djilkibaev (Sov. J. Nucl. Phys. 49(2), 384 (1989))



Production Solenoid:

- 8 GeV Protons enter, pions produced, decay to muons
- Graded magnetic field reflects pions/muons to transport solenoid

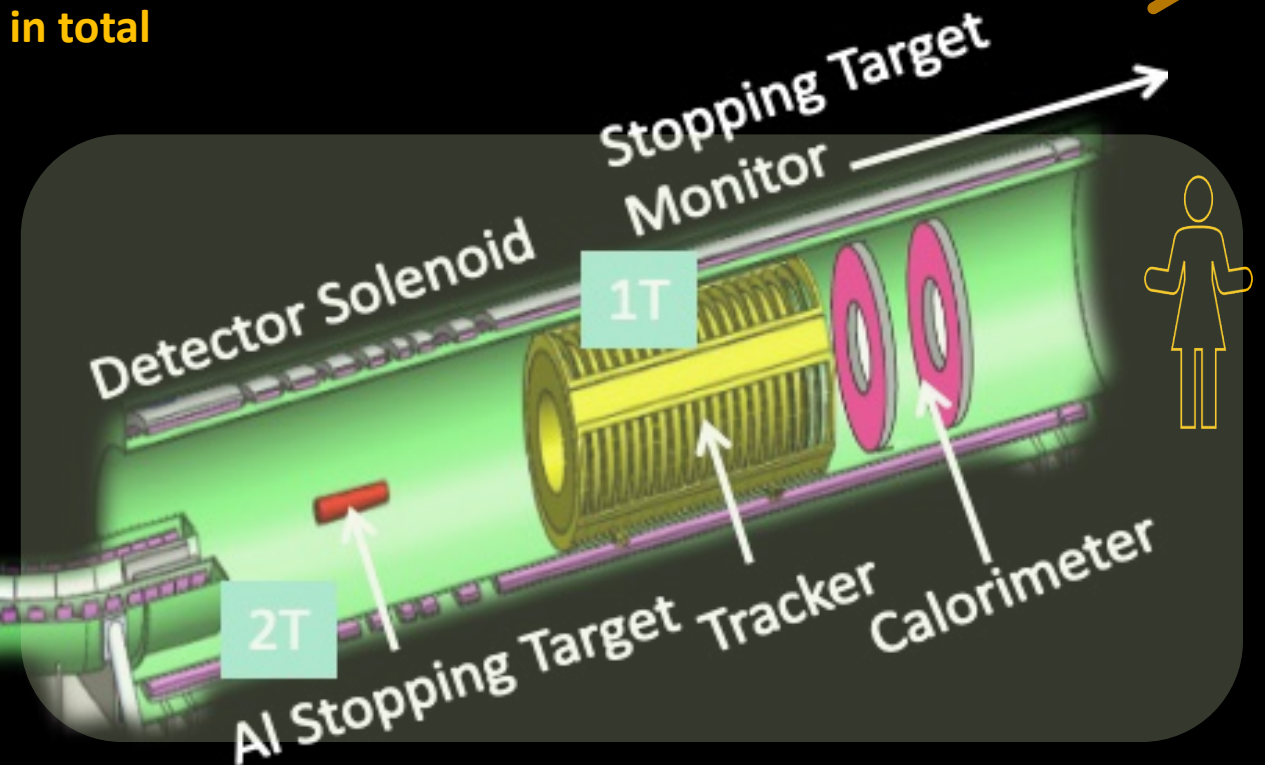
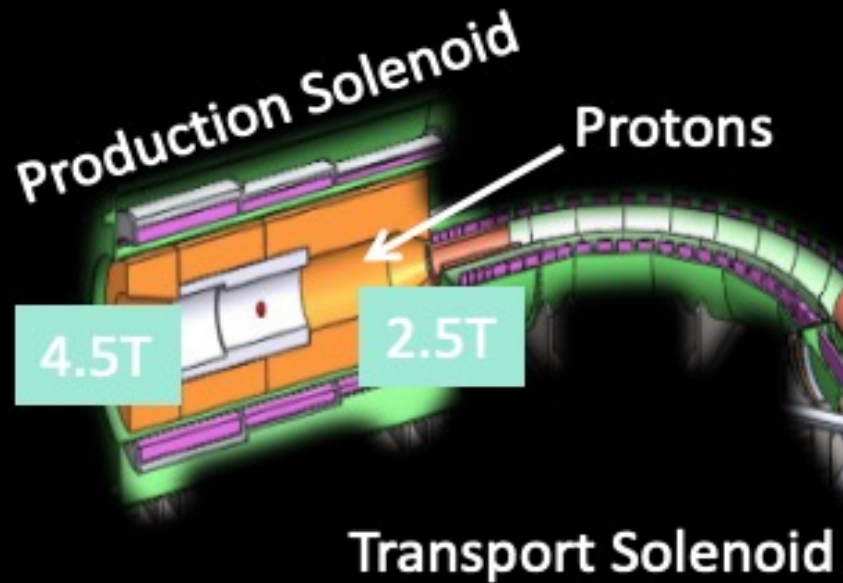
Transport Solenoid:

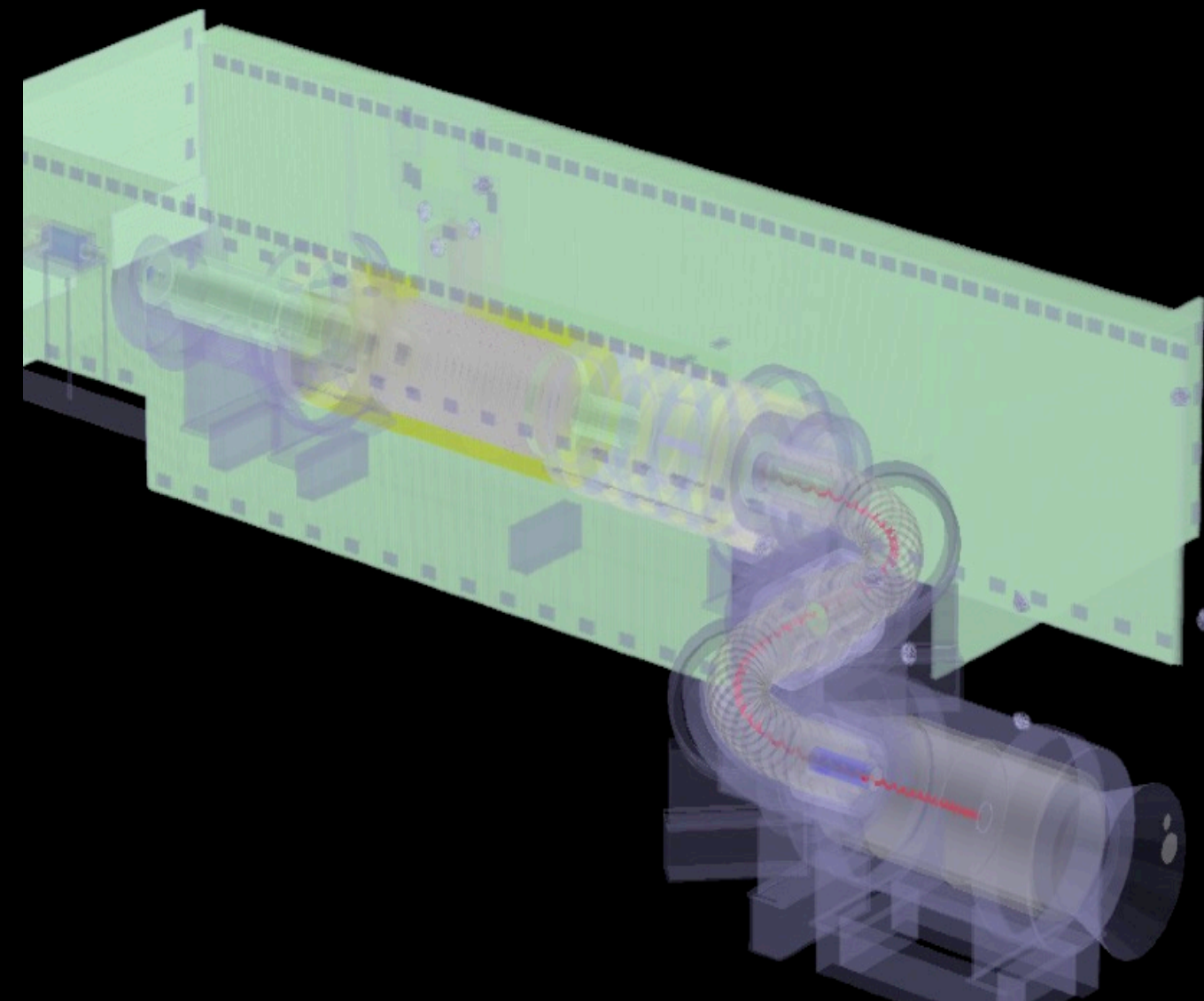
- "S" shape removes line of sight backgrounds
- Windows remove anti-protons
- Collimators help select low momentum, negative muons and "focus" on detector solenoid aperture.

Detector Solenoid:

- Al Stopping Target made of thin foils captures the muons
- Graded magnetic field "focusses" electrons on tracker
- Straw tracker and calorimeter measure momentum

25 m in total





Beamline & Solenoids: Status

What is the current status of the beamline components?

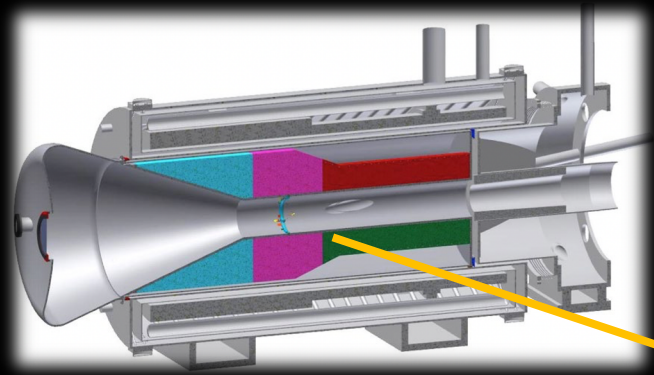
Beamline: Status



The beamline installation is almost complete:

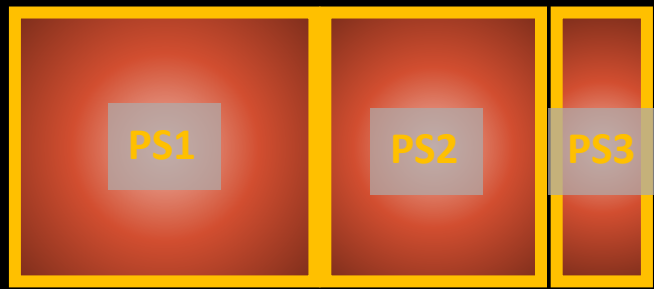
- Vacuum System installed
- Instrumentation upstream of diagnostic absorber in progress

Production Solenoid: Status

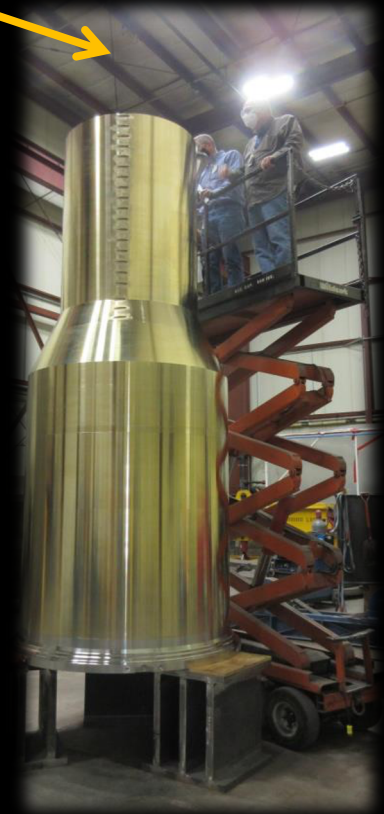


All 3 coils fabricated, under-going tests at vendor

Heat & Radiation Shield



Production Target & Frame

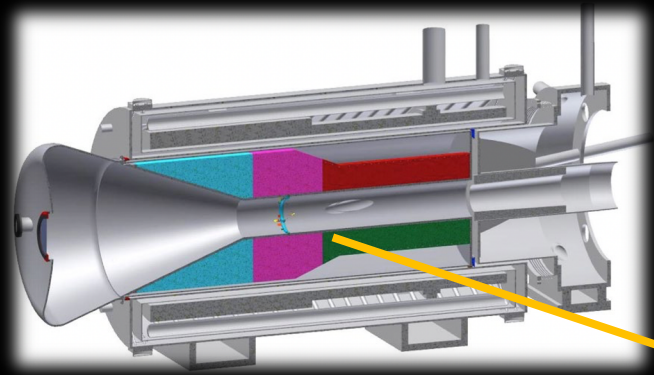


<https://www.symmetrymagazine.org/article/a-robot-ballet>

Nice video of robotic extraction of target

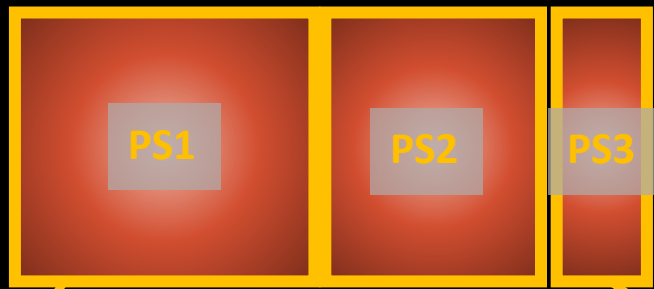


Production Solenoid: Status

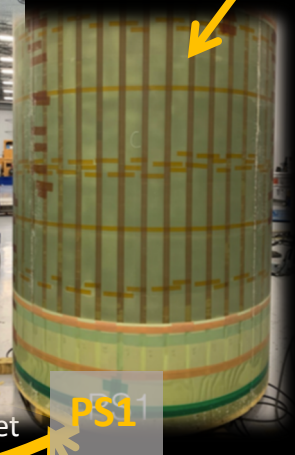
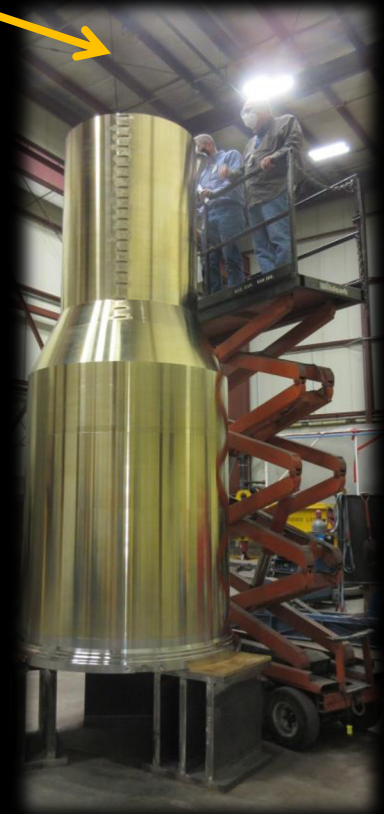


All 3 coils fabricated, under-going tests at vendor

Heat & Radiation Shield



Production Target & Frame



PS1



PS2 inserted into shell



PS3

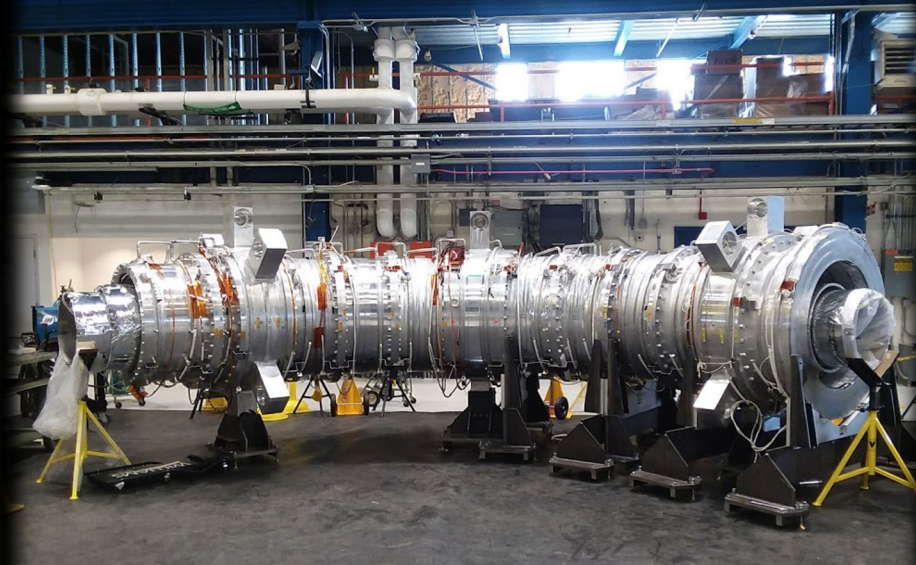
<https://www.symmetrymagazine.org/article/a-robot-ballet>

Nice video of robotic extraction of target

Transport Solenoid: Status



Thermal shield shown next to TSu



TS coldmass at Fermilab awaiting final tests.



Both TSu and TSd are at FNAL

- All coils of the TS are now at Fermilab.
- TSu and TSd cold-masses assembled.
- Testing almost complete
- Outer thermal shield will be split and re-assembled around the TSu cold-mass alongside in image.



TSd vacuum vessel, awaiting leak check



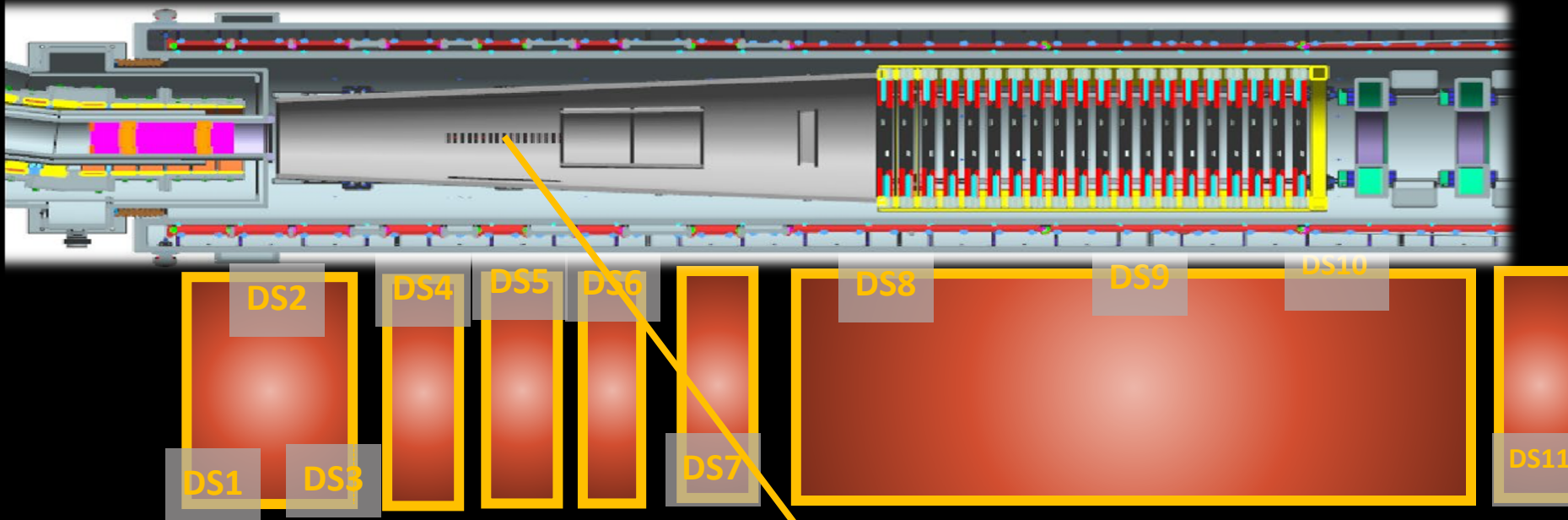
TSu vacuum vessel, leak tight



Nice video of the TS being lifted at FNAL in July:

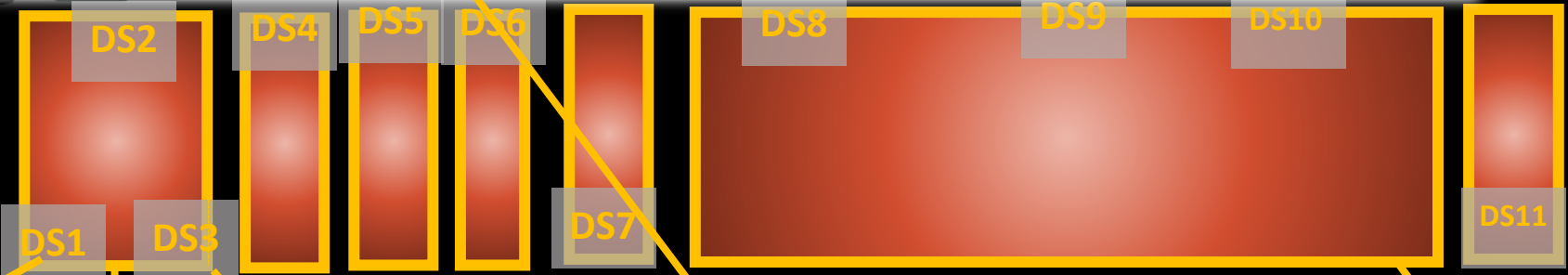


Detector Solenoid: Status



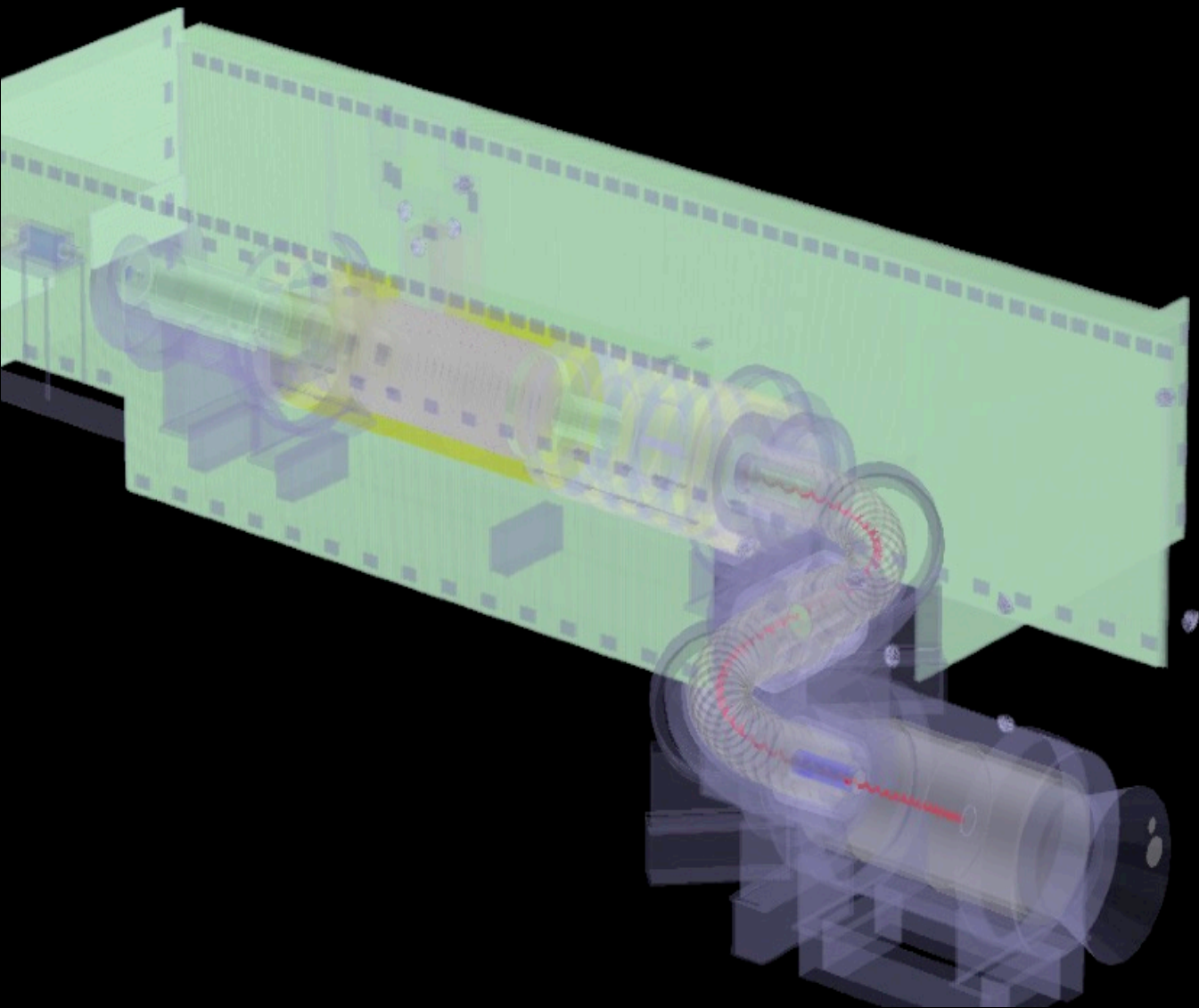
Aluminum stopping target in frame

Detector Solenoid: Status



4/11 coils fabricated, continuing at vendor





“Background free” design

How do we ensure Mu2e is “background free”?
Why have we designed our detectors in this way?



Removing Backgrounds

Beam delivery and detector systems optimized for high intensity, pure muon beam – must be “background free”:

- Intrinsic :

- Scale with number of stopped muons.

- Late arriving :

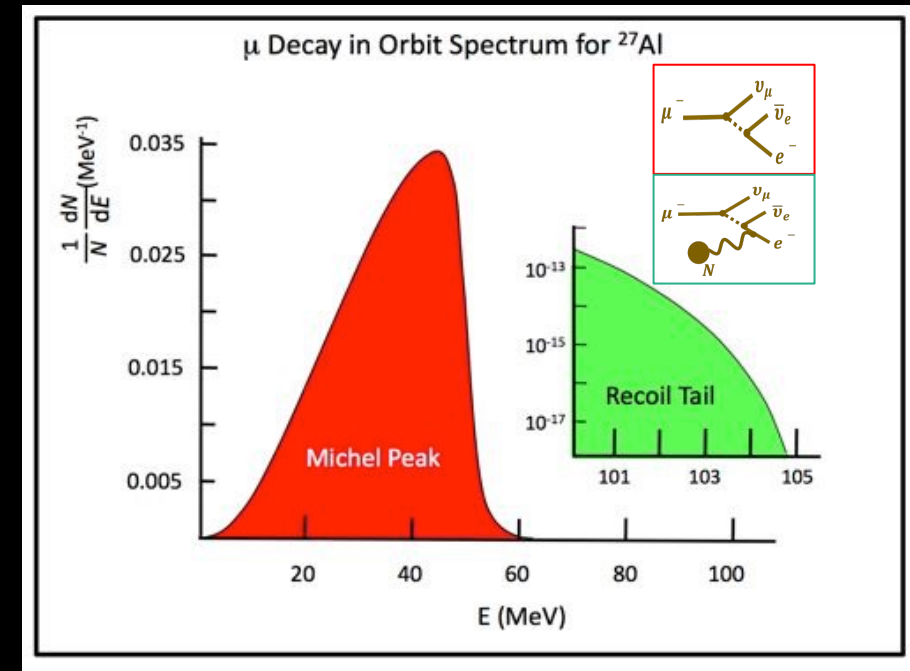
- Scale with number of late protons/ extinction performance

Type	Source	Mitigation	Yield (over lifetime of experiment)
Intrinsic	Decay in Orbit (DIO)	Tracker Design/ Resolution	0.144 ± 0.028 (stat) ± 0.11 (sys)
Late Arriving	Pion Capture	Beam Structure /Extinction	0.021 ± 0.001 (stat) ± 0.002 (sys)
	Pion Decay in Flight	-	$0.001 \pm < 0.001$
Other	Anti-proton	Thin Absorber Windows	0.04 ± 0.022 (stat) ± 0.020 (sys)
	Cosmic Rays	Active Veto System	0.209 ± 0.0022 (stat) ± 0.055 (sys)

Muon Decay-in-Orbit (DIO) Backgrounds



- In Aluminium 39% of stopped muons will decay in orbit (DIO):
 - Free muon decay: peak electron energy far below our signal energy (peaks 52.8 MeV).

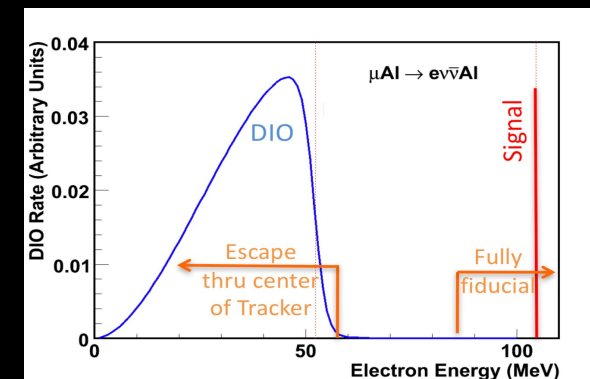
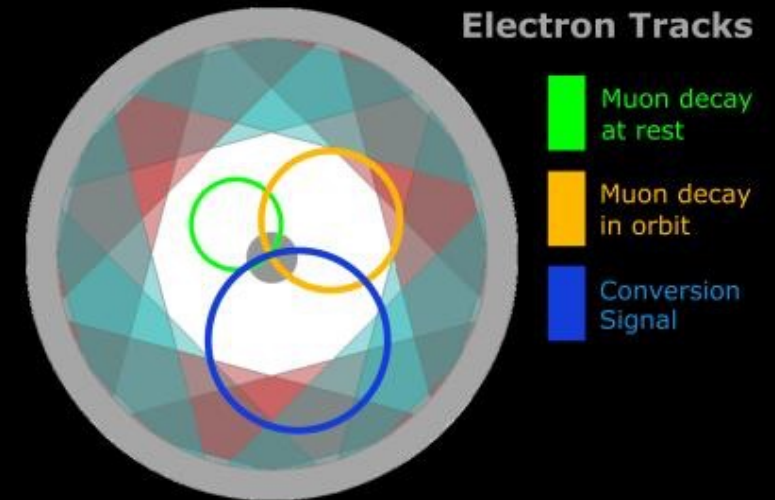




Muon Decay-in-Orbit (DIO) Backgrounds

- In Aluminium 39% of stopped muons will decay in orbit (DIO):
 - Free muon decay: peak electron energy far below our signal energy (peaks 52.8 MeV).
- Charged particles in a magnetic field follow helical paths. The radius is determined by the particle's momentum:
 - **Annular Design** → Excludes low momentum electrons via hollow centre:
 - Inner 38 cm un-instrumented .
 - Reduces need to reject $\sim 10^{18}$ to $\sim 10^5$.
 - Blind to > 99% of DIO spectrum.

Transverse Plane



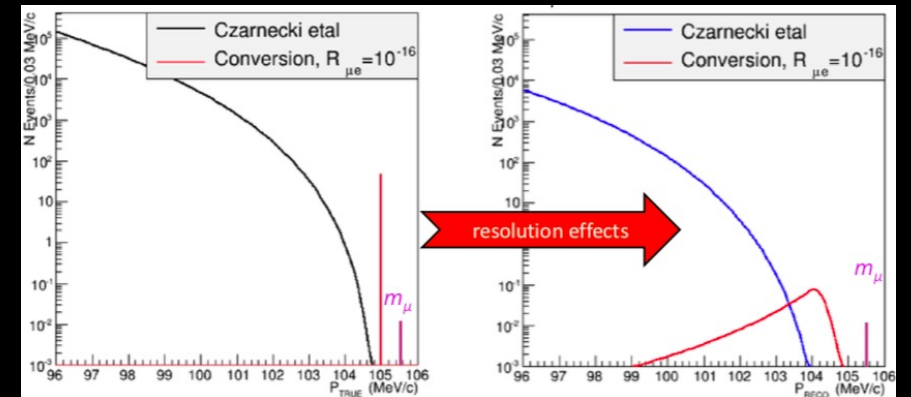
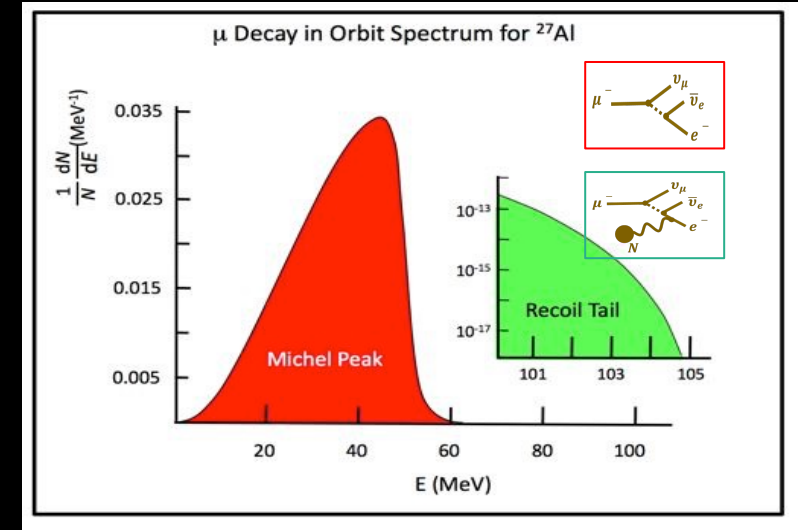


Muon Decay-in-Orbit (DIO) Backgrounds

- In Aluminium 39% of stopped muons will decay in orbit (DIO):
 - Free muon decay: peak electron energy far below our signal energy (peaks 52.8 MeV).
 - If muon is bound in atomic orbit, the outgoing electron can exchange momentum with the nucleus.
 - Means there is a very small probability that an electron with energy close to that of a conversion electron can be produced
 - Recall that Mu2e will acquire ϑ (10^{20}) Protons on Target to achieve design goal

The differential energy spectrum of DIO electron spectrum has been parameterized in A. Czarnecki et al., "Muon decay in orbit: Spectrum of high-energy electrons," Phys. Rev. D 84 (Jul, 2011) .

- Necessitates tracker resolution of better than 200 KeV/c



Rejecting DIO Backgrounds



- To remove remaining DIOs momentum resolution < 200 KeV/c achieved by:



Rejecting DIO Backgrounds

- To remove remaining DIOs momentum resolution < 200 KeV/c achieved by:
 1. **Low Mass \rightarrow Minimizes scattering and energy loss :**
 - Entire Detector Solenoid held under vacuum ($\sim 10^{-4}$ torr).
 - Ultra low mass tracker.



Rejecting DIO Backgrounds

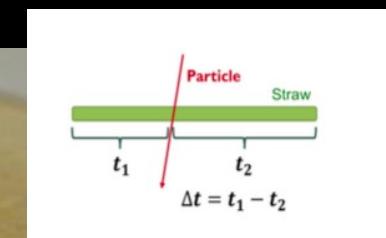
- To remove remaining DIOs momentum resolution < 200 KeV/c achieved by:
 1. **Low Mass** \rightarrow Minimizes scattering and energy loss :
 - Entire Detector Solenoid held under vacuum ($\sim 10^{-4}$ torr).
 - Ultra low mass tracker.
 2. **Segmented** \rightarrow Handle high rates and provide high-precision momentum measurements.

The Tracker: Design



- Tracker is constructed from self-supporting panels of low mass straws tubes detectors
- 18 stations, 2 planes per station, 6 panels per plane, 96 straws per panel.
- Straw drift tubes aligned transverse to the axis of the Detector Solenoid.
 - 1m, 5 mm diameter straw
 - Walls: 12 mm Mylar + 3 mm epoxy
 - 25 mm Au-plated W sense wire
 - 33 – 117 cm in length
 - 80:20 Ar:CO₂ with HV < 1500 V
 - Straw wall thickness of 15 μm has never been done before
- Charged particles ionize gas – drift to wire – detect signals!

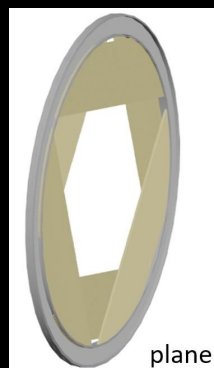
The Straws:



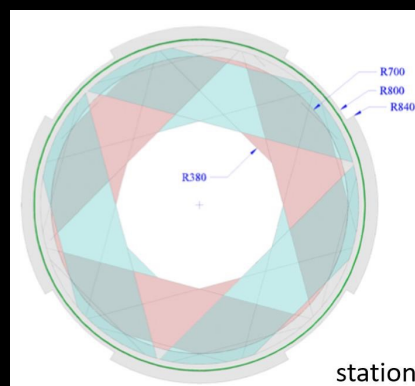
Panels



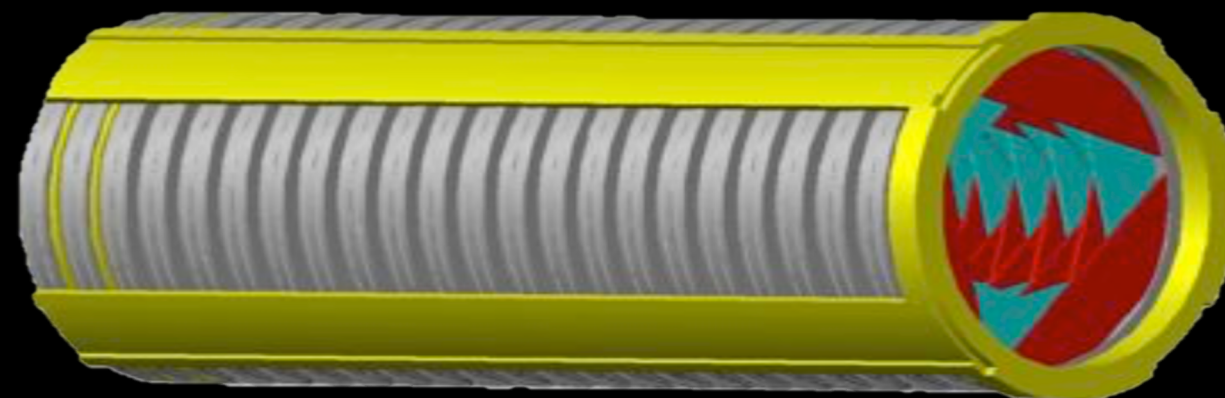
Plane



Station



The Tracker: ~ 3m, 1 T field





Rejecting DIO Backgrounds

- To remove remaining DIOs momentum resolution < 200 KeV/c achieved by:
 1. **Low Mass** \rightarrow **Minimizes scattering and energy loss** :
 - Entire Detector Solenoid held under vacuum ($\sim 10^{-4}$ torr).
 - Ultra low mass tracker.
 2. **Segmented** \rightarrow **Handle high rates and provide high-precision momentum measurements.**



Rejecting DIO Backgrounds

- To remove remaining DIOs momentum resolution < 200 KeV/c achieved by:
 1. **Low Mass** \rightarrow **Minimizes scattering and energy loss** :
 - Entire Detector Solenoid held under vacuum ($\sim 10^{-4}$ torr).
 - Ultra low mass tracker.
 2. **Segmented** \rightarrow **Handle high rates and provide high-precision momentum measurements.**
 3. **Sophisticated reconstruction algorithm containing:**
 1. hit construction,
 2. time clustering,
 3. tracking via pattern recognition,
 4. refinement via Kalman fitting,
 5. background rejection via Machine Learning

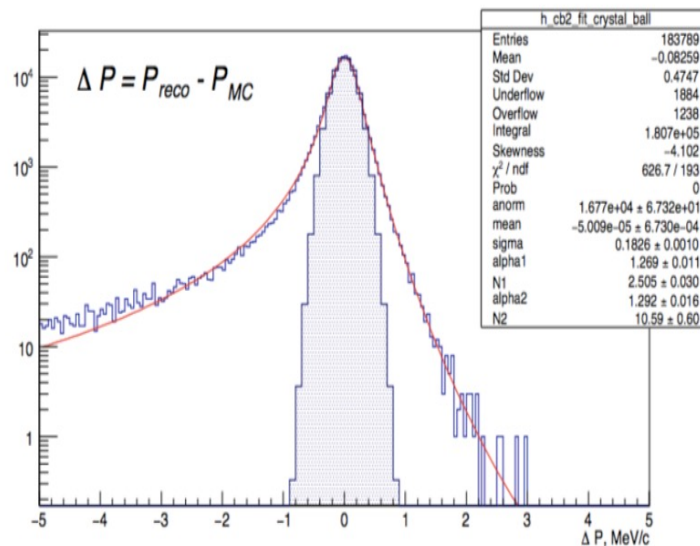
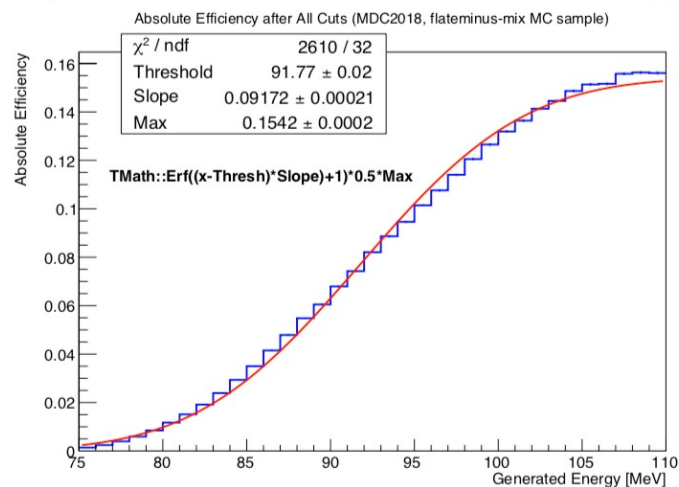
Acceptance & Response

Paper documenting our Machine Learning analysis.
<https://arxiv.org/abs/2106.08891>



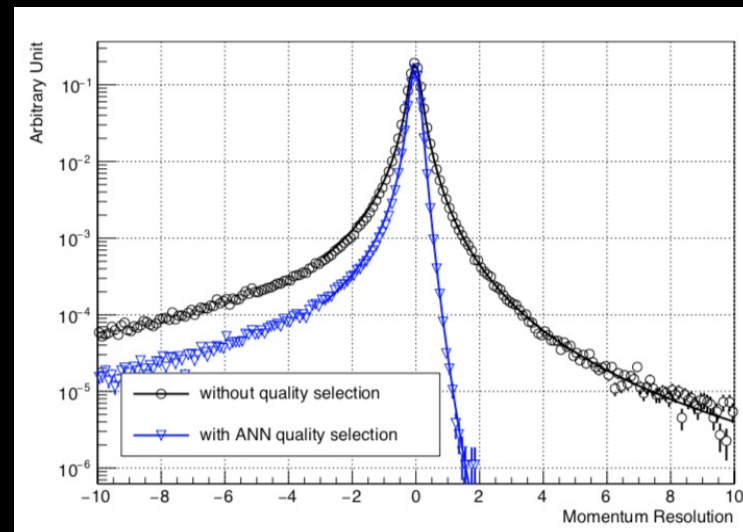
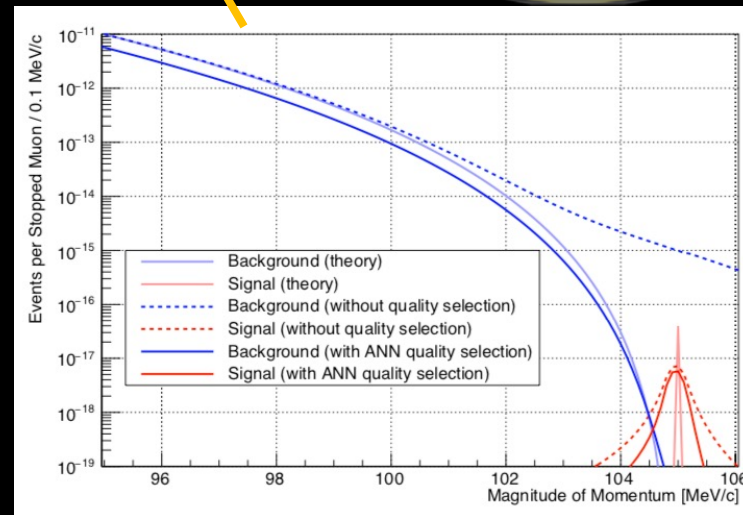
- Experiment is “blind” to anything with energy < 75 MeV.
- Tracking resolution improved by use of ANN.

Absolute Efficiency (as function of generated energy)



Resolution (core) : 183 keV ie $\frac{\sigma(p)}{p} \sim 0.2\%$ at 100 MeV

Non Gaussian tail $\sim 4\%$





Removing Backgrounds

Beam delivery and detector systems optimized for high intensity, pure muon beam – must be “background free”:

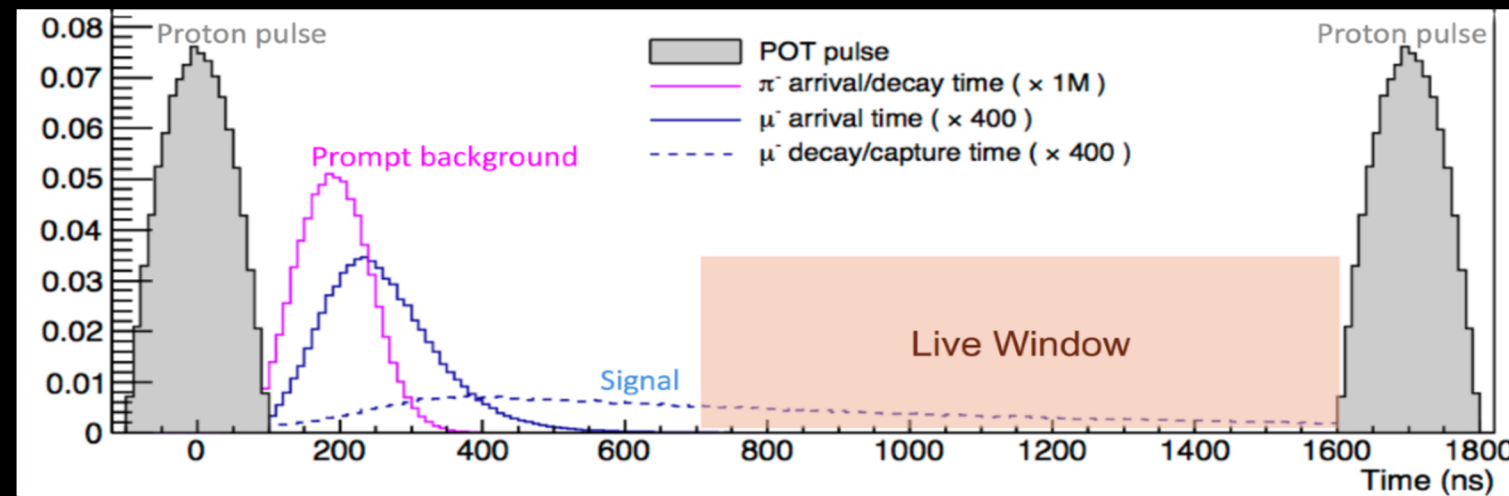
- Intrinsic :
 - Scale with number of stopped muons.
- Late arriving :
 - Scale with number of late protons/ extinction performance

Type	Source	Mitigation	Yield (over lifetime of experiment)
Intrinsic	Decay in Orbit (DIO)	Tracker Deign/ Resolution	0.144 ± 0.028 (stat) ± 0.11 (sys)
Late Arriving	Pion Capture	Beam Structure /Extinction	0.021 ± 0.001 (stat) ± 0.002 (sys)
	Pion Decay in Flight	-	$0.001 \pm < 0.001$
Other	Anti-proton	Thin Absorber Windows	0.04 ± 0.022 (stat) ± 0.020 (sys)
	Cosmic Rays	Active Veto System	0.209 ± 0.0022 (stat) ± 0.055 (sys)



Pion Backgrounds

- Pions – have a free lifetime of 26ns. They decay to produce muons (and neutrinos). Muons can further decay and produce backgrounds.
- Eliminate prompt backgrounds using a primary beam of short proton pulse. Use a delayed measurement window (~ 700 ns after proton pulse at target). Before this point we ignore any tracks we see in our detector systems.

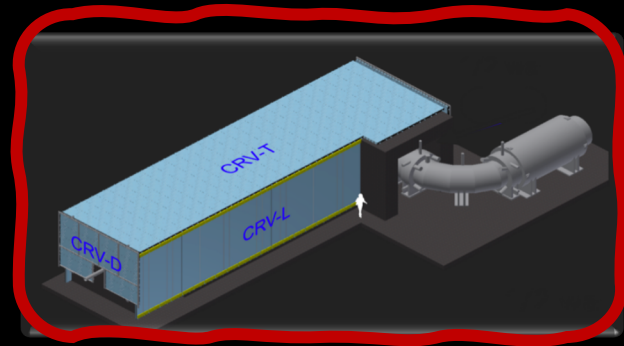


- Out-of-time pions could fall inside “livegate” but are eliminated by excellent extinction in our proton beam.
- **We require an out-of-time/in time protons $< 10^{-10}$.**



Removing Backgrounds

Beam delivery and detector systems optimized for high intensity, pure muon beam – must be “background free”:



Active veto system surrounds detector region

Type	Source	Mitigation	Yield (over lifetime of experiment)
Intrinsic	Decay in Orbit (DIO)	Tracker Design/Resolution	0.144 ± 0.028 (stat) ± 0.11 (sys)
Late Arriving	Pion Capture	Beam Structure /Extinction	0.021 ± 0.001 (stat) ± 0.002 (sys)
	Pion Decay in Flight	-	$0.001 \pm < 0.001$
Other	Anti-proton	Thin Absorber Windows	0.04 ± 0.022 (stat) ± 0.020 (sys)
	Cosmic Rays	Active Veto System	0.209 ± 0.0022 (stat) ± 0.055 (sys)

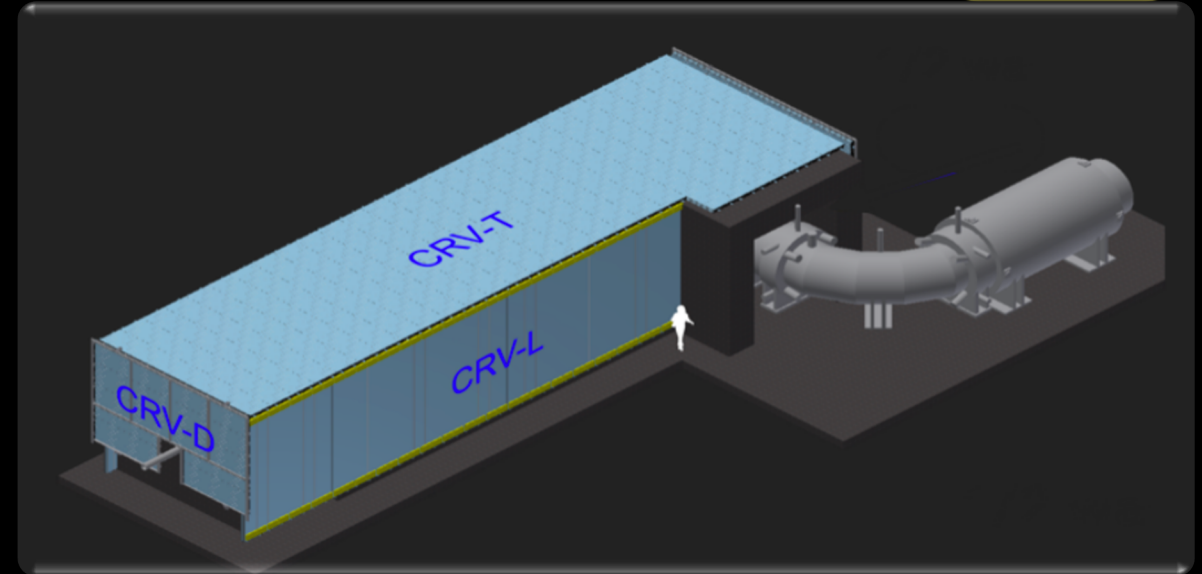
The Cosmic Ray Veto

Each day, ~ 1 conversion-like electron is produced by cosmic rays

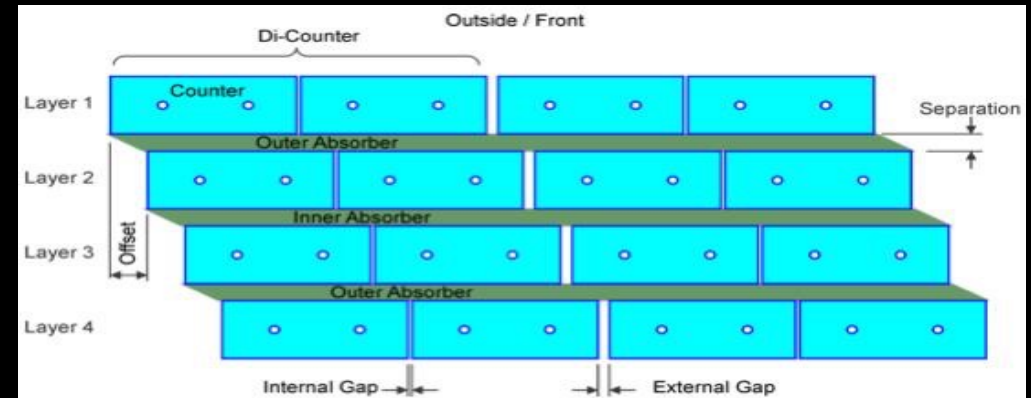
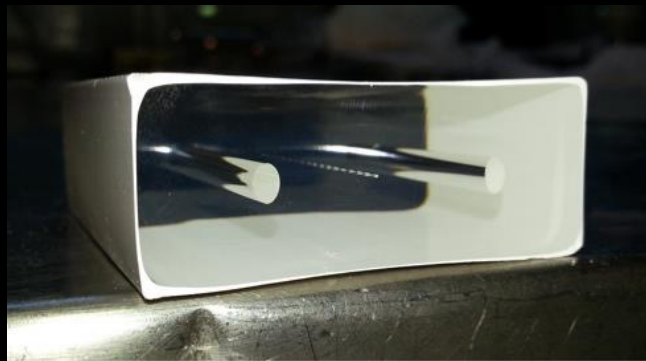


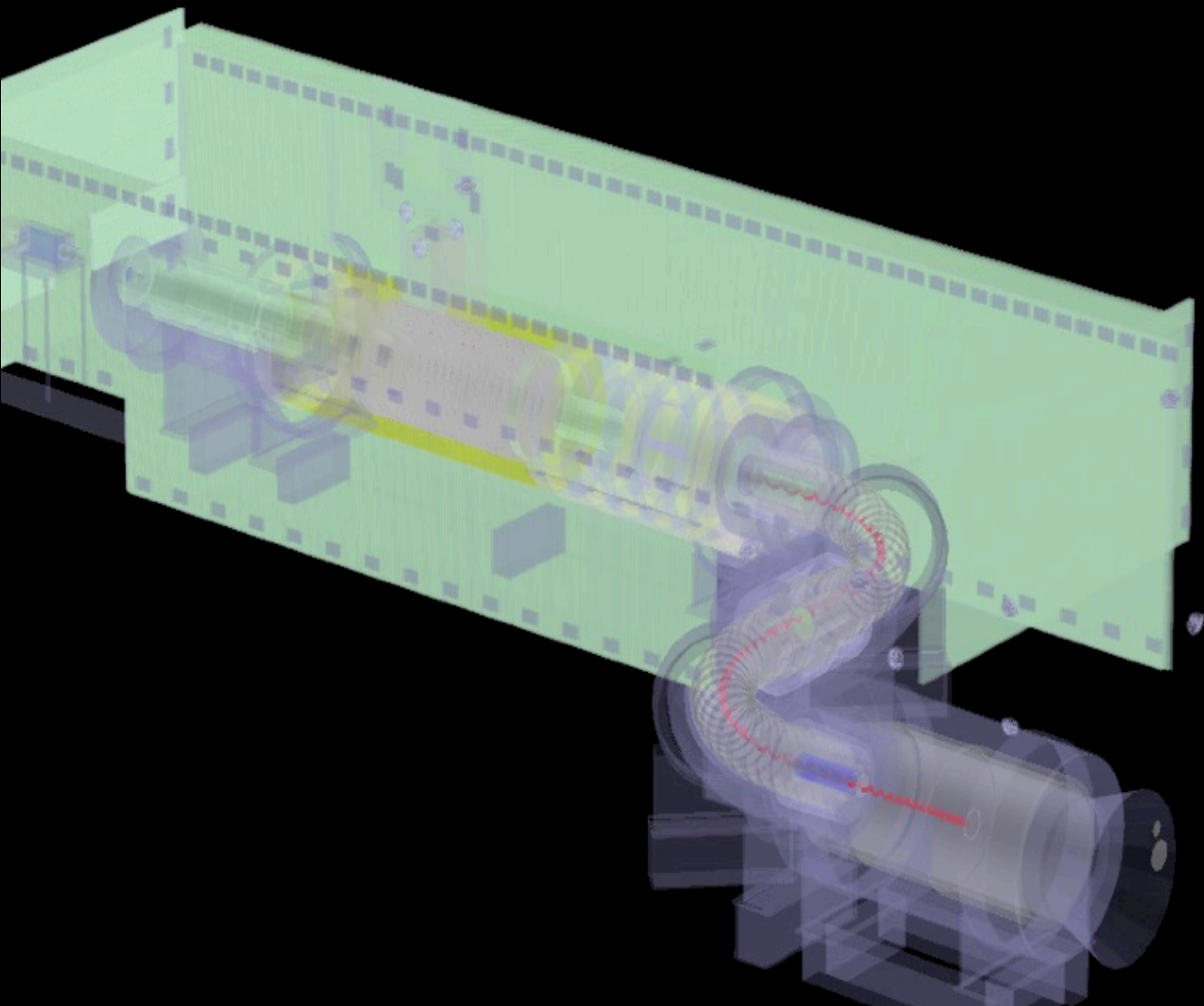
Cosmic Ray Veto will prevent cosmic muons faking a signal:

- 4 layers of extruded polystyrene scintillator counter.
- Surrounds the top and sides of DS and the downstream end of the Transport Solenoid.
- Suppresses the spurious detection of conversion-like particles initiated by cosmic-ray muons.
- 99.99% efficiency requirement!



Each panel is composed of $5 \times 2 \times 450 \text{ cm}^3$ scintillator bars:





Building our Detectors

- How are our detectors constructed?
- Where are they constructed?
- What is the current status of each system?
- When will Mu2e be ready?

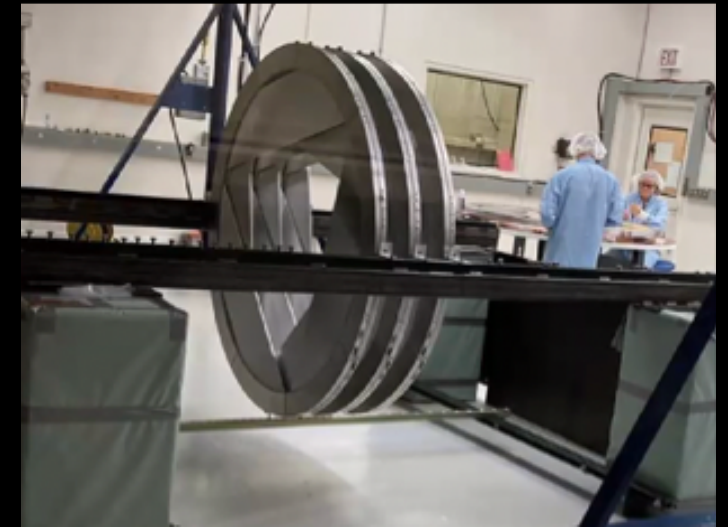
The Tracker: Progress



2020: Production at University of Minnesota, testing at Duke Uni., → Over 60% of panels fabricated, and passed tests

2021: Assembly at FNAL

→ 6/36 planes so far assembled on site

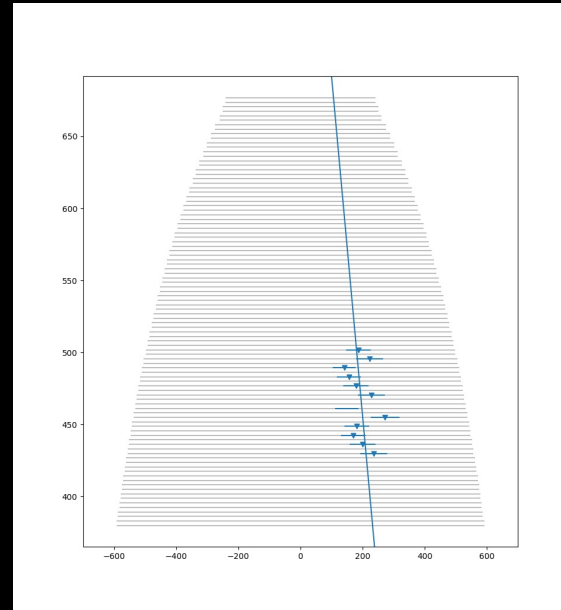
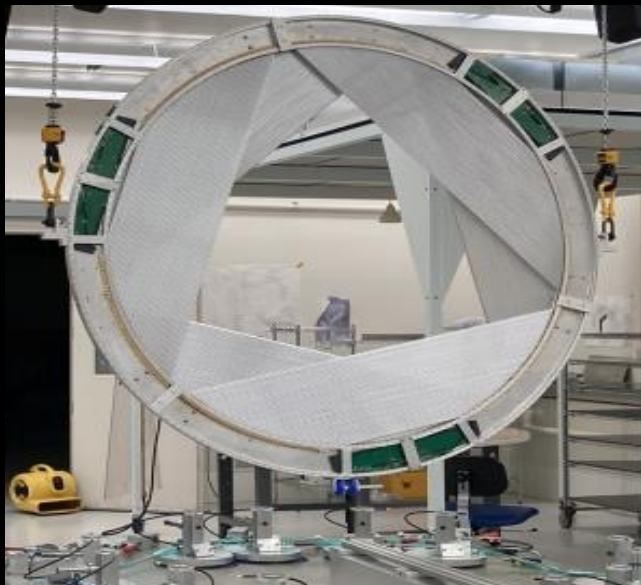
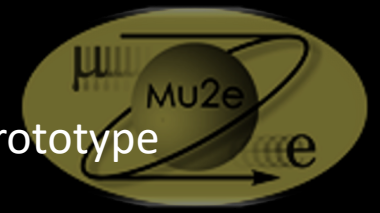


Vacuum tests at FNAL, here for single panel.



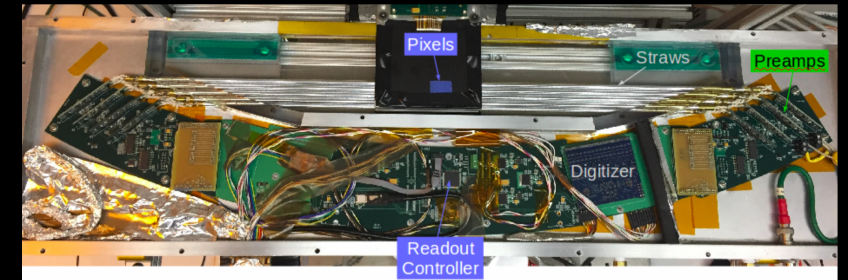
The Tracker: Progress

2020: Vertical Slice Test begins at FNAL

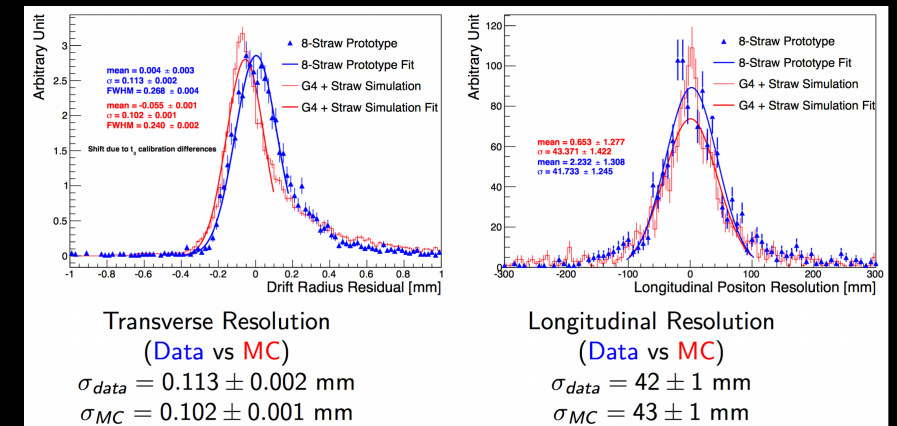


- Use Cosmic Rays.
- Use information gained to update MC.
- Measured performance and resolutions.
- First test with real data.

2017-2018: Electronics prototype produced at LBNL



Measured gain, crosstalk, resolution...



8 channel prototype

→ Good agreement between MC/Data

→ Resolution can be achieved

The Calorimeter

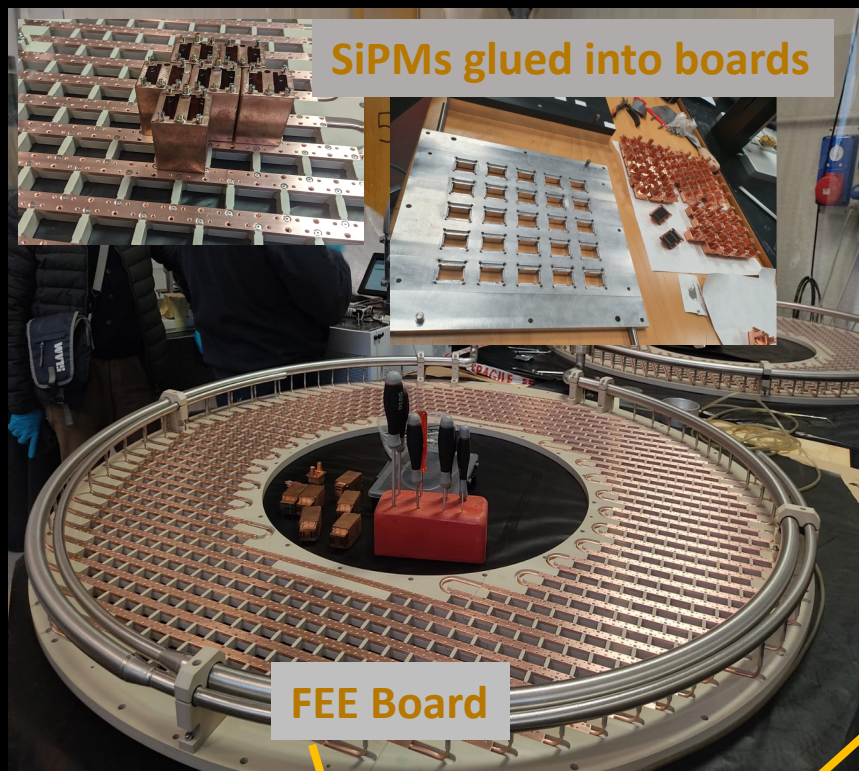
All parts ready
Assembly beginning now



Inner Ring



Outer Ring



SiPMs glued into boards

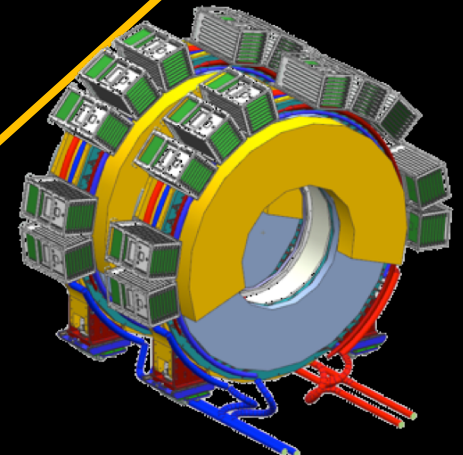
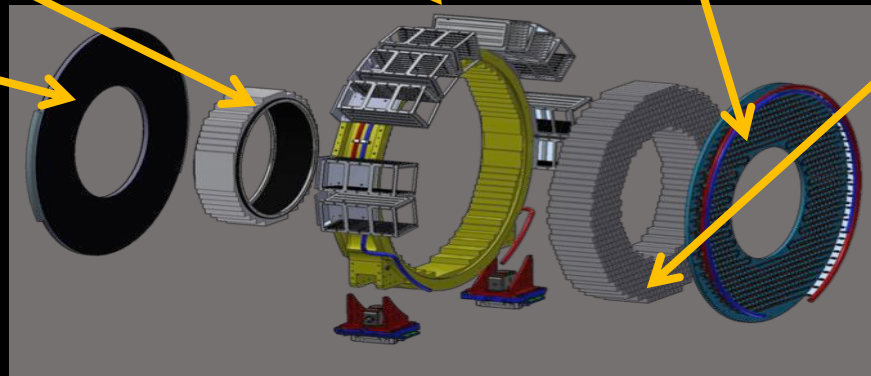
FEE Board



Crystals at FNAL in sealed cupboard after QA.



Source Calibration System



Me at FNAL – finishing crystals QA (2020)

The Cosmic Ray Veto System

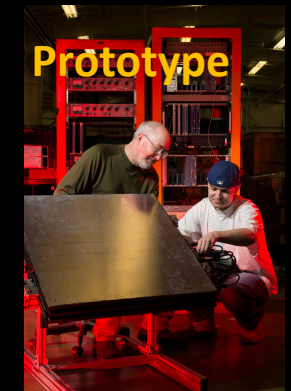


Modules at Argonne

- 56/83 modules fabricated at UVA
- Electronics production underway
- Front-End-Boards produced KSU
- Vertical slice test underway



2020: Vertical Slice Test at UVA



The Stopping Target Monitor (STM)



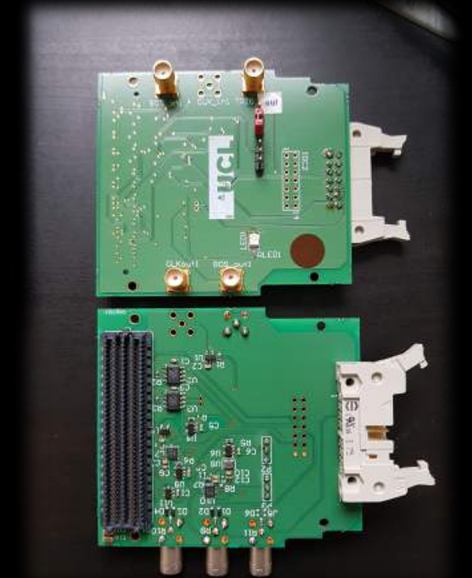
- Need an accurate measure of total number of stopped muons in the target (within 10%) .
- Placed far downstream of Detector Solenoids (~34 m from target).
- STM uses HPGe and LaBr₃ detectors to measure X/gamma-rays produced by stopped muons in Al target:
 1. Prompt X-ray emitted from muonic atoms at 347keV;
 2. Delayed gamma ray at 844keV;
 3. Semi-prompt gamma ray at 1.809MeV.

HPGe and LaBr detectors procured

$$R_{\mu e} = \frac{\Gamma(\mu^- + A(Z,N) \rightarrow e^- + A(Z,N))}{\Gamma(\text{all-captures})} < 7 \times 10^{-13} (90\% \text{C.L})$$



2019: Test stands setup to begin DAQ development



Test beam at ELBE this year... results being analyzed



Mu2e: Timeline



Sept. 2021 Mu2e construction is nearly complete:

- Beamline is finished.
- TS on-site and finalizing testing, PS and DS testing and fabrication on-going at vendor.
- Tracker straws, FEE prototypes, calorimeter crystals and SiPMs, STM detectors, and CRV counters are complete.
- Assembly and testing of these detector components is on-going.



Mu2e: Timeline

2022 → Transition to installation

Sept. 2021 Mu2e construction is nearly complete:

- Beamline is finished.
- TS on-site and finalizing testing, PS and DS testing and fabrication on-going at vendor.
- Tracker straws, FEE prototypes, calorimeter crystals and SiPMs, STM detectors, and CRV counters are complete.
- Assembly and testing of these detector components is on-going.



Mu2e: Timeline

2022 → Transition to installation

Late 2022 → Start Detector commissioning
(e.g. in situ cosmic ray data taking)

Sept. 2021 Mu2e construction is nearly complete:

- Beamline is finished.
- TS on-site and finalizing testing, PS and DS testing and fabrication on-going at vendor.
- Tracker straws, FEE prototypes, calorimeter crystals and SiPMs, STM detectors, and CRV counters are complete.
- Assembly and testing of these detector components is on-going.

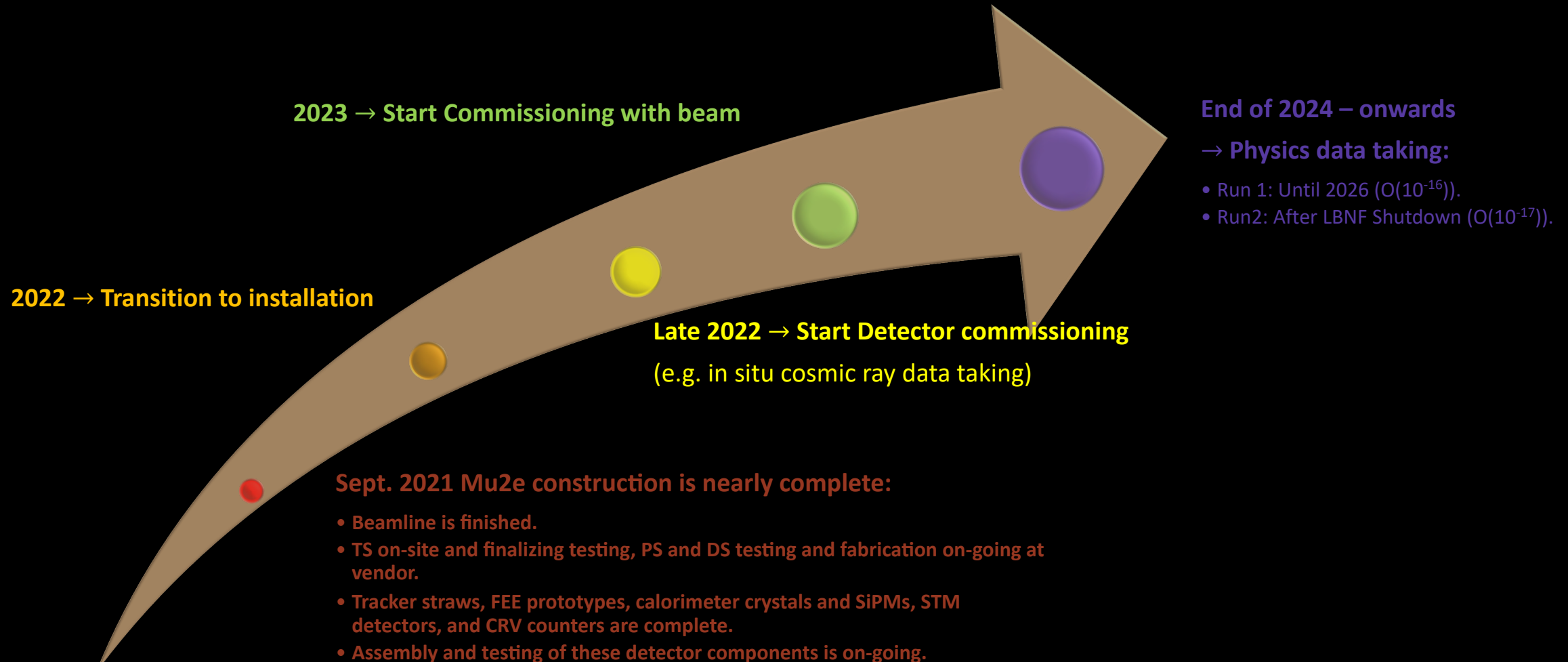


Mu2e: Timeline





Mu2e: Timeline



Mu2e Sensitivity

Paper published soon.



Run 1:

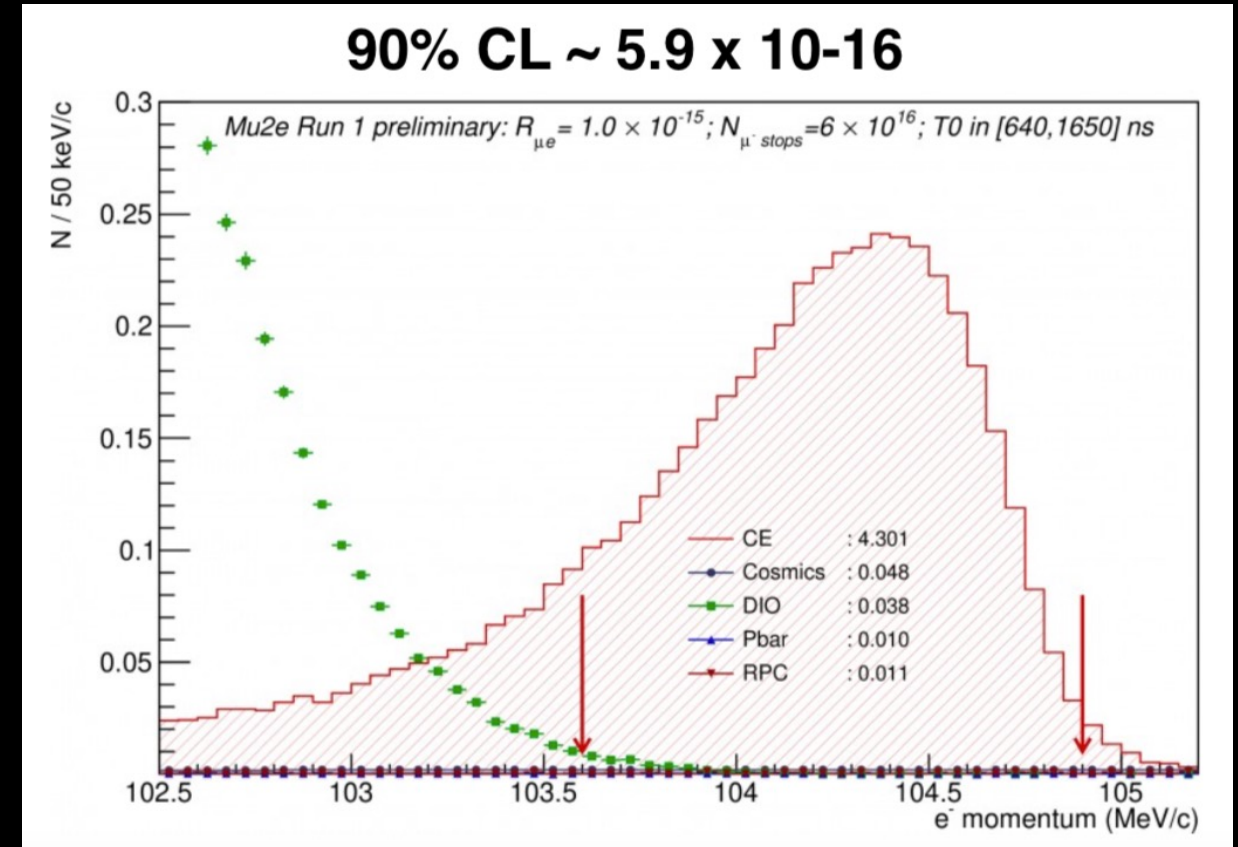
- Beam on target in late by 2024

Run1: 2024-2026:

- 10^3 improvement over SINDRUM-II 90% CL limit
- PIP-II/LBNF shutdown scheduled for end of 2026

Run2: Data-taking resumes early 2029

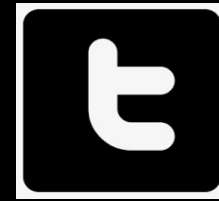
- The goal is a $\times 10^4$ improvement over SINDRUM-II: (90% CL)



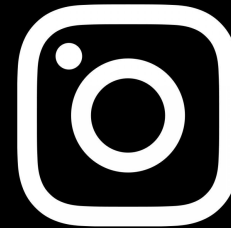
Follow us



Watch the experiment evolve with frequent videos and images:



<https://twitter.com/Mu2eExperiment>



<https://www.instagram.com/mu2eexperiment/>





Summary

- Muon CLFV channels offer deep indirect probes into BSM.
- Mu2e is at the forefront of active global CLFV program. Discovery potential over a wide range of well motivated BSM models.
- Muon-to-electron sector complements tau and Higgs collider searches such as: $\tau \rightarrow e\gamma$ or $\mu\gamma$ and $H \rightarrow e\tau, \mu\tau$, or μe .
- It is important to eliminate Standard Model backgrounds so the experiment is designed to be “background free”:
 - Super conducting solenoids to collect and efficiently transport low momentum muons;
 - Pulsed beam removes backgrounds from pions;
 - Low mass, annular tracker has high resolution to avoid DIO backgrounds;
 - Cosmic Ray Veto surrounds detectors to remove “fake signals” from Cosmic muons.

Thank You for listening!



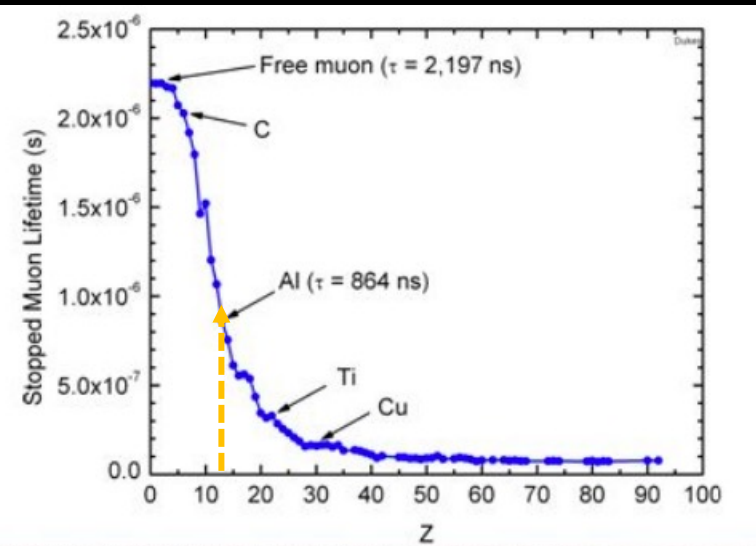
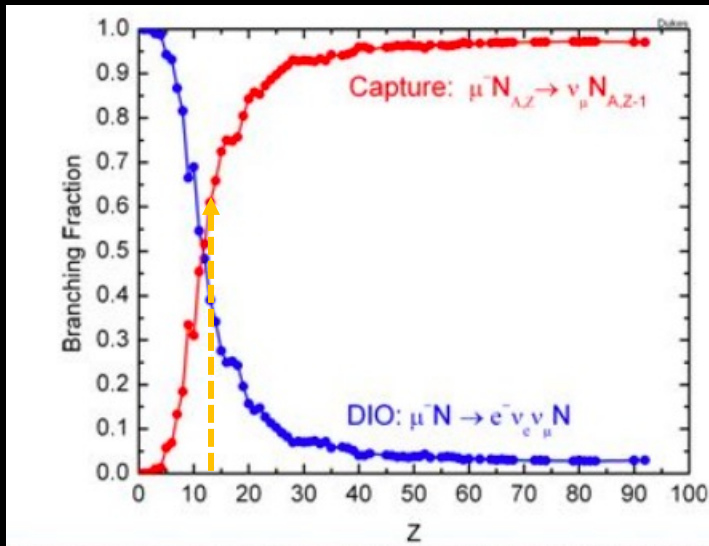
Useful Resources

1. S. T. Petcov, Sov. J. Nucl. Phys. **25**, 340 (1977); Yad. Fiz. **25**, 1336 (1977) [erratum].
2. S. M. Bilenky, S. T. Petcov, and B. Pontecorvo, Phys. Lett. B **67**, 309 (1977).
3. W. J. Marciano and A. I. Sanda, Phys. Lett. B **67**, 303 (1977).
4. B. W. Lee, S. Pakvasa, R. E. Shrock, and H. Sugawara, Phys. Rev. Lett. **38**, 937 (1977); **38**, 1230 (1977) [erratum].
5. J. Adam *et al.* (EG Collaboration), Phys. Rev. Lett. **110**, 20 (2013).
6. W. Bertl *et al.* (SINDRUM-II Collaboration), Eur. Phys. J. **C47**, 337 (2006).
7. U. Bellgardt *et al.*, (SINDRUM Collaboration), Nucl. Phys. **B299**, 1 (1988).
8. A.M. Baldini *et al.*, “MEG Upgrade Proposal”, arXiv:1301.7225v2 [physics.ins- det].
9. Y. Kuno *et al.*, “COMET Proposal” (2007) see also <https://arxiv.org/abs/1812.09018> for Phase I TDR
10. Mu2e TDR, arXiv:1501.05241
11. Nuclear Physics B - Proceedings Supplements Volumes 248–250, March–May 2014, Pages 35-4
12. A. Czarnecki *et al.*, “Muon decay in orbit: Spectrum of high-energy electrons,” Phys. Rev. D 84 (Jul, 2011) .
13. Sindrum-II “Improved limit of Branching Fraction of $\mu^- \rightarrow e^+$ in Titanium”, Phys Lett B 422 (1998) 334-338 (1998)



Why Aluminum?

Practical Advantages	Physics Advantages
Chemically Stable	Conversion energy such that only tiny fraction of photons produced by muon radiative capture.
Available in required size/shape/thickness	Muon lifetime long compared to transit time of prompt backgrounds.
Low cost	Conversion rate increases with atomic number, reaching maximum at Se and Sb, then drops. Lifetime of muonic atoms decreases with increasing atomic number.
	Lifetime of muonic atom sits in “goldilocks” region i.e. neither longer than 1700 ns pulse spacing and greater than our pionic live gate.



The lifetime of a muon in a muonic atom decreases with increasing atomic number.

Complementarity in Target Materials

$$BR(\mu \rightarrow e) \propto |DC_{DL} + S^p C_{S,L}^p + V^p C_{V,R}^p + S^n C_{S,L}^n + V^n C_{V,R}^n|^2 + (L \leftrightarrow R)$$

	S	D	V ¹	V ²
$\frac{B(\mu \rightarrow e, Ti)}{B(\mu \rightarrow e, Al)}$	$1.70 \pm 0.005_y$	1.55	1.65	2.0
$\frac{B(\mu \rightarrow e, Pb)}{B(\mu \rightarrow e, Al)}$	$0.69 \pm 0.02_{\rho_n}$	1.04	1.41	$2.67 \pm 0.06_{\rho_n}$

y = nuclear scalar form factor, ρ_n = nuclear neutron density

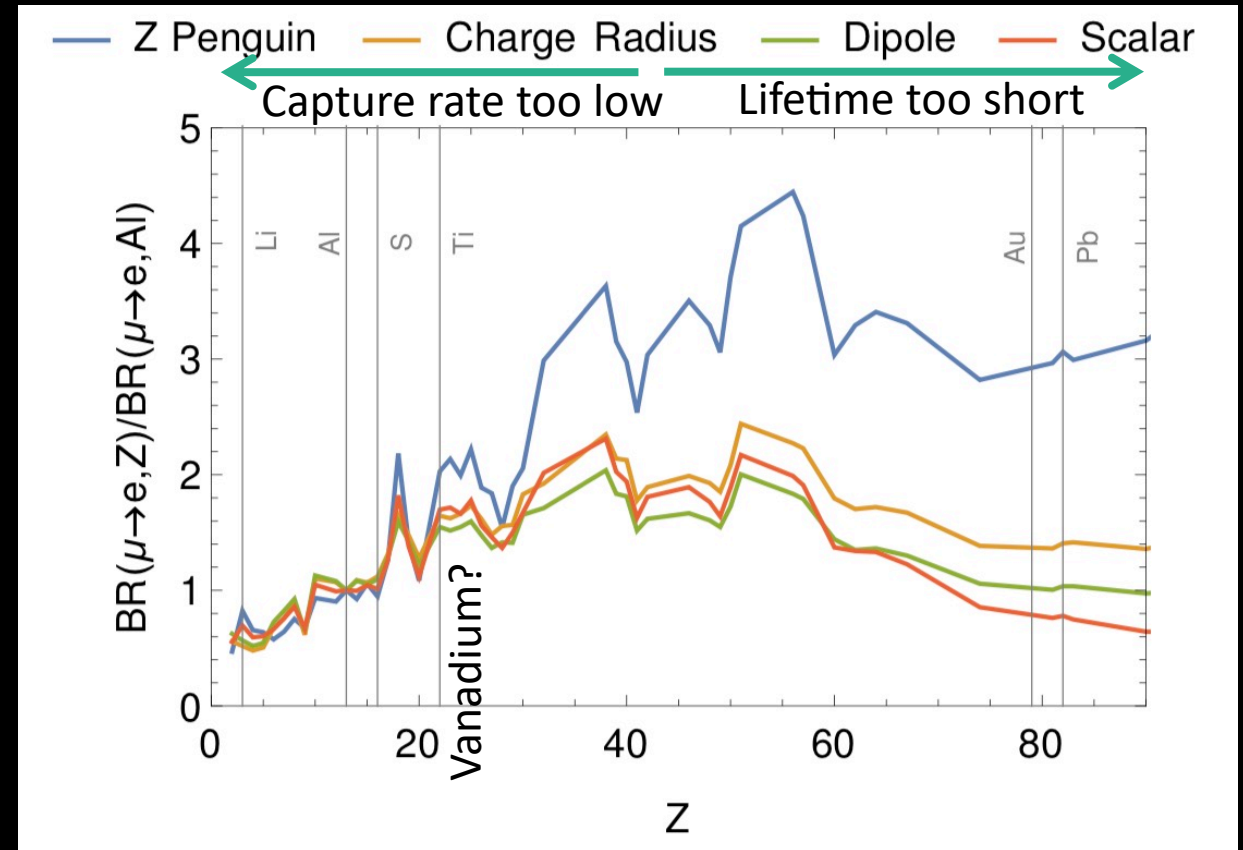
V. Cirigliano, S. Davidson, Y. Kuno, Phys. Lett. B 771 (2017) 242
 S. Davidson, Y. Kuno, A. Saporta, Eur. Phys. J. C78 (2018) 109
 Kitano et al 2002

If we do see a signal in Al:

- Various operator coefficients add coherently in the amplitude.
- Weighted by nucleus-dependent functions.

→ Requires measurements of conversion rate in other target materials!

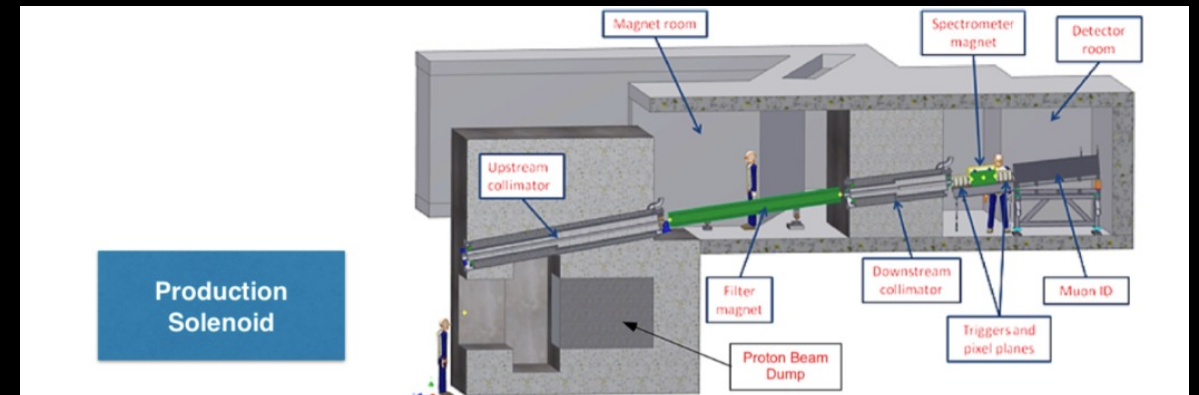
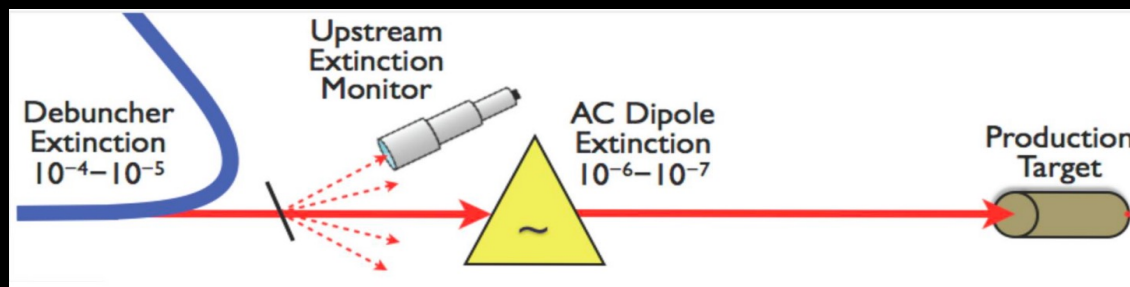
- Need to choose a target which is sensitive to directions Al is “blind” to



Removing out-of-time protons



- Must have out-of-time : in-time proton ratio must be kept $< 10^{-10}$ to remove potential backgrounds.
- 2 phase process:
 - Fast “kicker” which transfers the proton beam from the Recycler to the Delivery Ring preserves extinction.
 - Extinction of 10^{-5} is expected as the proton beam is extracted and delivered.
 - The beam line from the Delivery Ring to the production target has a set of AC oscillating dipoles that sweep out-of-time protons into a system of collimators. This should achieve an additional extinction of 10^{-7} or better.
- Extinction measured using a detector system: Si-pixel + sampling EMC .





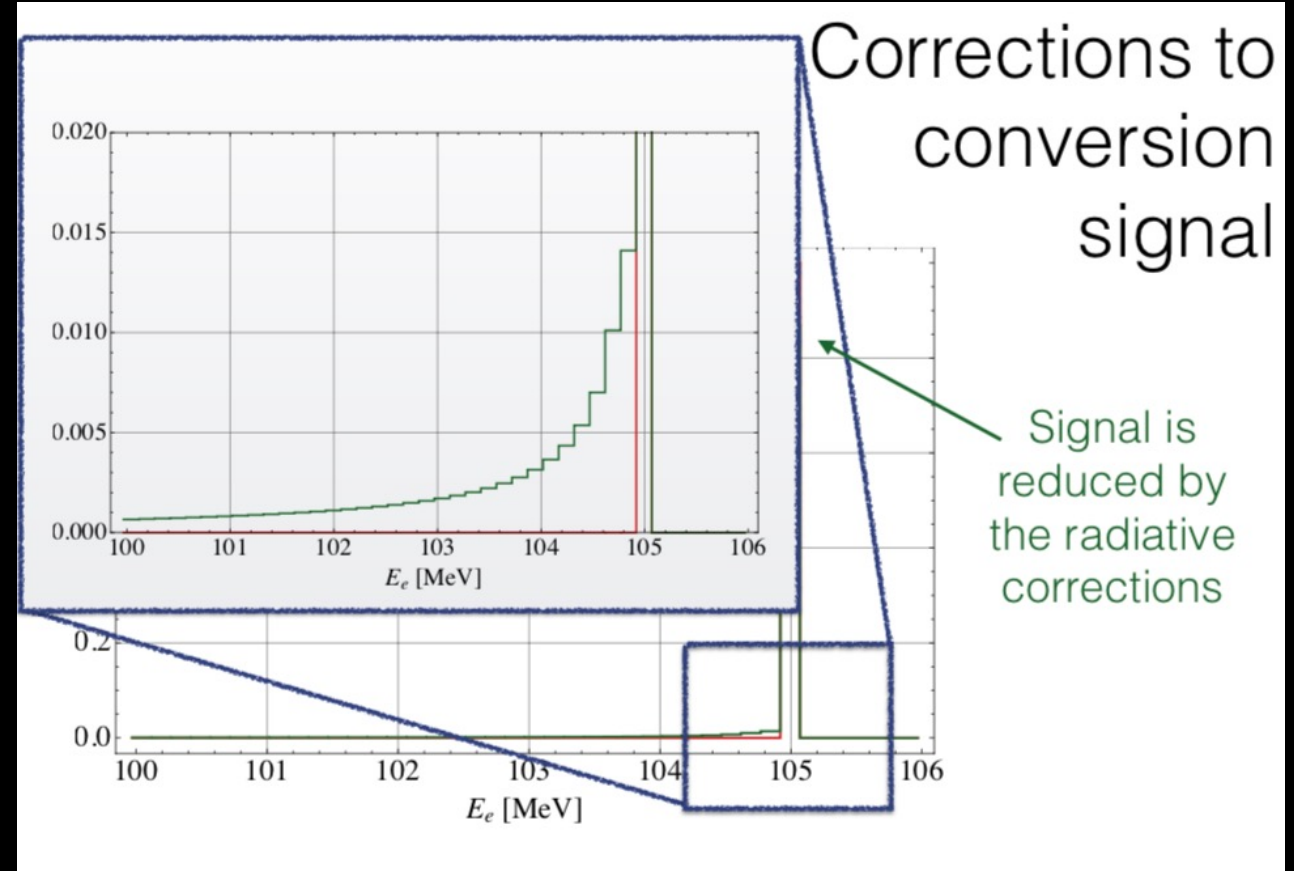
Radiative Corrections for CE Signal

- Our signal also requires radiative corrections:

$$\frac{m_\mu}{\Gamma_0} \frac{d\Gamma}{dE_e} = \frac{\alpha}{2\pi} \left[\left(\ln \frac{4E_e^2}{m_e^2} - 2 \right) \frac{E_e^2 + m_\mu^2}{m_\mu (m_\mu - E_e)} + P(E_e) \right]_+$$

Universal part; proportional to the splitting function
Model dependent part (polynomial in electron energy)

Only the leading order in $Z\alpha$





g-2 Result: Implications for Mu2e

P. Paradisi / Nuclear Physics B (Proc. Suppl.) 248–250 (2014)

- Dipole transitions $\mu \rightarrow e\gamma$ in the leptonic sector are accounted for by means of the effective Lagrangian :

$$\mathcal{L} = e \frac{m_\ell}{2} \left(\bar{\ell}_R \sigma_{\mu\nu} A_{\ell\ell'} \ell'_L + \bar{\ell}'_L \sigma_{\mu\nu} A_{\ell\ell'}^* \ell_R \right) F^{\mu\nu},$$

$$\frac{\text{BR}(\ell \rightarrow \ell' \gamma)}{\text{BR}(\ell \rightarrow \ell' \nu_\ell \bar{\nu}_{\ell'})} = \frac{48\pi^3 \alpha}{G_F^2} \left(|A_{\ell\ell'}|^2 + |A_{\ell'\ell}|^2 \right).$$

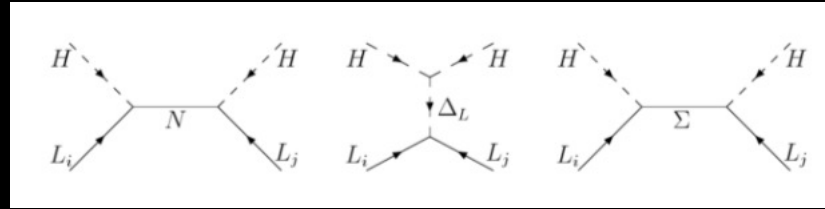
- The underlying $\mu \rightarrow e\gamma$ transition can also generate lepton flavor conserving processes like the anomalous magnetic moments (Δa_μ) as well as leptonic electric dipole moments (EDMs, d_μ).

- In terms of the effective Lagrangian can write as :

$$\Delta a_\ell = 2m_\ell^2 \text{Re}(A_{\ell\ell}), \quad \frac{d_\ell}{e} = m_\ell \text{Im}(A_{\ell\ell}).$$

- On general grounds, one would expect that, in concrete NP scenarios, (Δa_μ), d_μ and $\text{BR}(\mu \rightarrow e\gamma)$, are correlated. In practice, their correlations depend on the unknown flavor and CP structure of the NP couplings and thus we cannot draw any firm conclusion.
- So g-2 result doesn't really effect us, but is suggests muons are doing something weird i.e. BSM which helps our physics case to explore ways BSM modes in the muon sector!

Origins of Neutrino Mass



- See Saw Models can induce rates which are not suppressed by smallness of these masses.
- For the Majorana case expect other contributions to the CLFV rates. Majorana masses require the existence of new states with their own masses
- There are 3 ways of inducing $\Delta L = 2$ Majorana neutrino masses from the tree level exchange of a heavy particle: from the exchange of right-handed neutrinos N_i (seesaw of type-I), of a scalar triplet Δ_L (type-II) and of fermion triplets Σ_i (type-III).
- Knowledge of the neutrino mass matrix is not sufficient to be able to distinguish between the 3 seesaw models. \rightarrow CLFV can help here.
- Type-II: The seesaw scalar triplet does not induce only the lepton number violating dimension 5 effective interaction. It also induces a lepton number conserving dimension 6 effective interaction which induces CLFV
- The dim-6 contribution could be many orders of magnitude larger than the dim-5 one, if the seesaw scale is relatively low, and if the smallness of the neutrino masses is due to a large part to the smallness of the $\mu\Delta/m\Delta$ parameter, one can get large rates.

Nuclear Physics B (Proc. Suppl.) 248–250 (2014) 13–19

Origins of Neutrino Mass

- Type-I:
 - All CLFV processes are necessarily induced at the loop level
 - Rates are not monotonous functions of m_N . Depend on nuclei considered. This illustrates how important it would be to search for $\mu \rightarrow e$ conversion, not only with one nuclei, but with several of them.
 - The reason why these rates vanish for a particular value of m_N can be traced back to the fact that the up quark and down quark contributions have different signs in the amplitude, depending on their different charges and weak isospins.

Nuclear Physics B (Proc. Suppl.) 248–250 (2014) 13–19

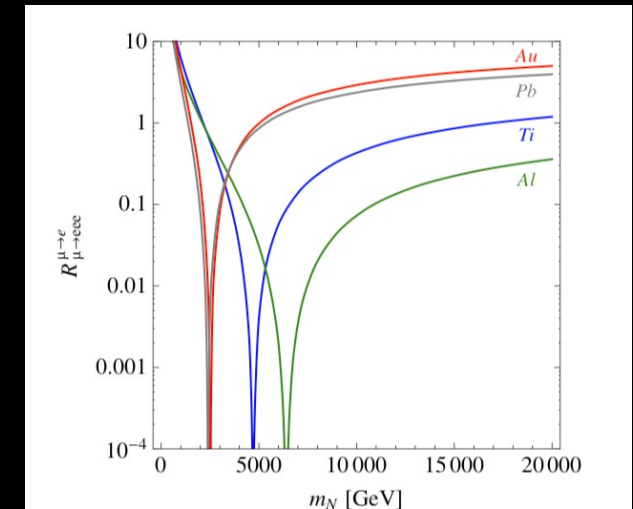
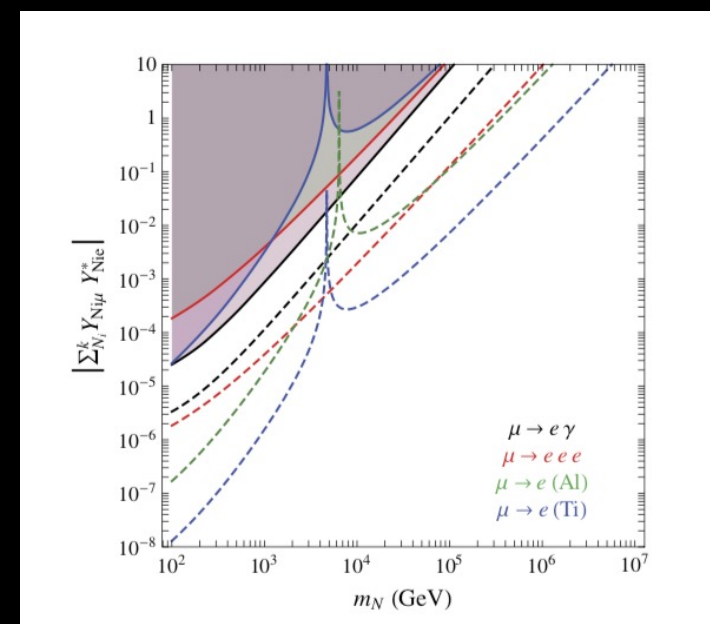


Figure 3: $R_{\mu \rightarrow e}^{\mu \rightarrow e} = R_{\mu \rightarrow e}^N / Br(\mu \rightarrow eee)$ as a function of the right-handed neutrino mass scale m_N , for $\mu \rightarrow e$ conversion in various nuclei, from Ref. [27].



Origins of Neutrino Mass

- Type-II:
 - $\mu \rightarrow eee$ at tree level, other processes can only be induced at one loop level. So $\mu \rightarrow eee$ has relatively higher rates.
 - For the ratio one does not always get a function which depends only on the seesaw state mass.
 - Ratios involving $\mu \rightarrow eee$ depend on the Yukawa coupling considerations

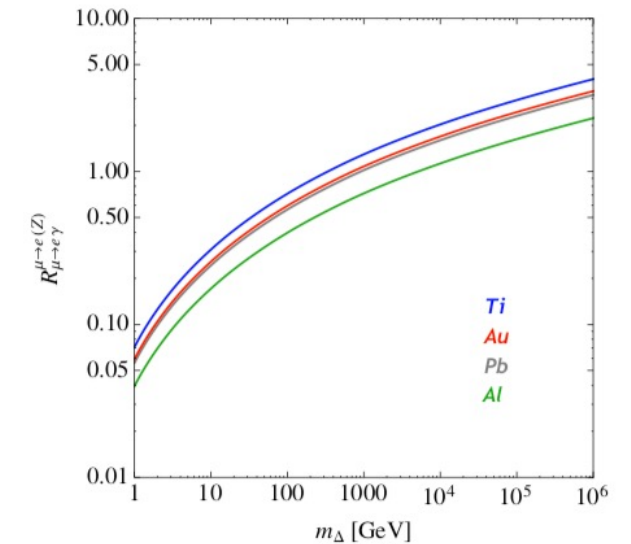


Figure 5: $R_{\mu \rightarrow e}^N / Br(\mu \rightarrow e\gamma)$ for various nuclei, as a function of m_{Δ} .

Nuclear Physics B (Proc. Suppl.) 248–250 (2014) 13–19



Origins of Neutrino Mass

- Type-III:
 - While in the type-I case there is flavor mixing only at the level of the neutral leptons, for the type-III case there is flavor mixing directly at the level of the charged leptons.
 - As a result, if for the type-I case all processes necessarily occurs at the loop level, for the type-III case the $\mu \rightarrow eee$ and $\mu \rightarrow e$ conversion process in atomic nuclei proceed at tree level.
 - However $\mu \rightarrow e \gamma$ occurs at loop level
 - Ratios are predicted to a fixed value!

Nuclear Physics B (Proc. Suppl.) 248–250 (2014) 13–19

COMET: Phased Implementation

